iScience

Article

Microbiota-derived β carotene is required for strobilation of *Aurelia aurita* by impacting host retinoic acid signaling

Graphical abstract

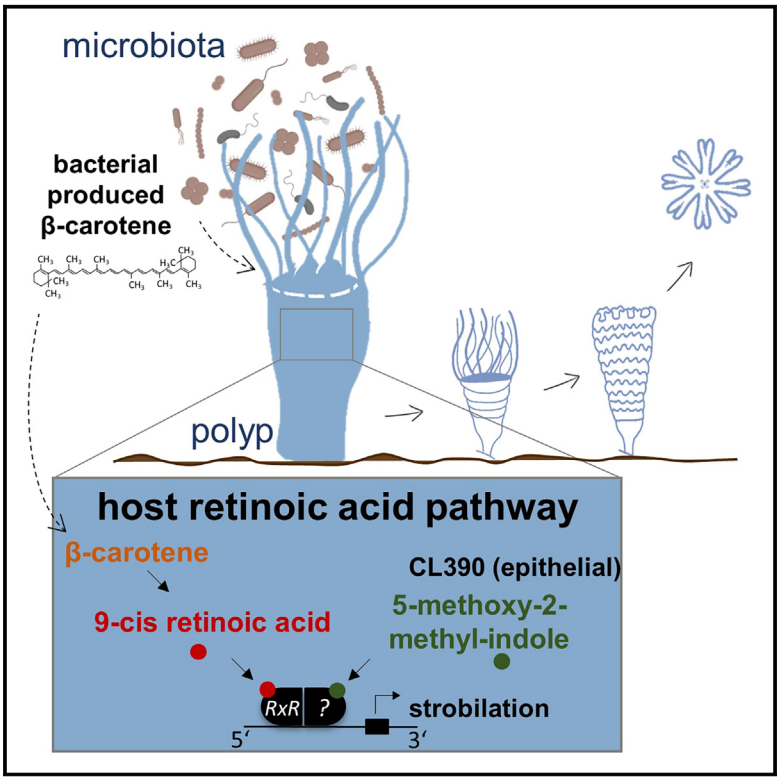

Highlights

- Bacterial-derived beta carotene modulates strobilation of *Aurelia aurita*
- RA genes undergo dynamic regulation impacted by bacterial-derived beta carotene
- A complex microbial community is required for strobilation success

Authors

Nadin Jensen, Nancy Weiland-Bräuer, Cynthia Maria Chibani, Ruth Anne Schmitz

Correspondence

rschmitz@ifam.uni-kiel.de

In brief

Biochemistry; Cell biology; Developmental biology; Microbiology

Jensen et al., 2025, iScience *28*, 111729
February 21, 2025
https://doi.org/10.1016/j.isci.2024.111729

CellPress

iScience

CellPress
OPEN ACCESS

Article

Microbiota-derived β carotene is required for strobilation of *Aurelia aurita* by impacting host retinoic acid signaling

Nadin Jensen,[1] Nancy Weiland-Bräuer,[1] Cynthia Maria Chibani,[1] and Ruth Anne Schmitz[1,2,*]
[1]Institute of General Microbiology, Christian-Albrechts University Kiel, Am Botanischen Garten 1-9, 24118 Kiel, Germany
[2]Lead contact
*Correspondence: rschmitz@ifam.uni-kiel.de
https://doi.org/10.1016/j.isci.2024.111729

SUMMARY

The strobilation process, an asexual reproduction mechanism in *Aurelia aurita*, transitions from the sessile polyp to the pelagic medusa stage. This study explored the essential role of the microbiome in strobilation, particularly through bacterial beta carotene's impact on the host's retinoic acid signaling pathway. Experiments demonstrated that native polyps undergo normal strobilation while sterile polyps exhibit morphological defects. Supplementing sterile polyps with provitamin A beta carotene or the vitamin A metabolite 9-cis retinoic acid (RA) remedied these defects, underscoring their crucial role in strobilation. Transcriptional analysis revealed that beta carotene and 9-cis RA restored expression of strobilation genes in sterile polyps to native levels. Inhibition of key enzymes in the RA pathway disrupted strobilation, further confirming its importance. The expression of bacterial β-carotenoid synthesis genes in the native microbiome, contrasted with tremendously reduced expression in antibiotic-treated polyps, emphasizes the microbiome's pivotal role in beta carotene provision, facilitating *A. aurita*'s strobilation through RA signaling.

INTRODUCTION

The concept of metaorganism has fundamentally transformed our understanding of the complex relationships between multicellular organisms and their associated microbial communities.[1–3] The associated microbiota plays a pivotal role in shaping fundamental aspects of the host, such as behavior and development.[2,4–6] In marine animals, particularly within the phylum Cnidaria, the microbiome influences developmental transitions[7–10] and the reproduction of their hosts.[11,12]

Drawing upon this understanding, the moon jellyfish *Aurelia aurita* offers valuable insights into the functional interactions between multicellular hosts and their microbiota, particularly during metamorphosis.[13,14] *A. aurita* undergoes a complex life cycle (see Figure 1), commencing with the release of planula larvae that settle and develop into sessile polyps resembling small cylindrical tubes. These polyps undergo significant morphological and developmental changes during strobilation, forming constrictions and generating an early strobila. These constrictions further develop and multiply, leading to the formation of brown-colored late strobila. Eventually, the segments detach from the strobila to become individual ephyrae, which then mature into free-swimming juvenile medusae. The characteristic adult medusae features are transparent, umbrella-shaped bells, and have delicate tentacles.[15–17] We recently demonstrated the pivotal role of the native microbiota in orchestrating the polyp-to-ephyra transition in *A. aurita* (Figure 1).[18,19] Our findings emphasized that the absence of microbes leads to a cessation in offspring generation. However, a detailed understanding of metamorphosis on the molecular level in *A. aurita*, Cnidarians in general, or several other invertebrates remains limited. In contrast, examining representatives such as insects and amphibians, which also undergo complex life cycles, reveals that metamorphosis is intricately regulated by host's neuronal and hormonal signals facilitated by nuclear hormone receptors.[20–23] In amphibians, thyroid-stimulating hormone (TSH) triggers tadpole-to-frog transformation via a thyroid hormone receptor (TR) and a retinoic X receptor (RxR) heterodimer, while in insects prothoracicotropic hormone (PTTH) and ecdysone activate metamorphosis genes through an ultraspiracles-ecdysone receptor (EcR) heterodimer.[24–27] Previous studies in *A. aurita* have highlighted similar potential regulators, such as retinoids (vitamin A derivates) and the RxR transcription factor, implicating the RxR involvement in transitioning from the polyp to medusa stage.[16] Upregulation of RxR during strobilation further suggested a significant role in strobilation.[16,19] Moreover, comparisons with other Cnidarian species showed a broader importance of retinoid signaling in jellyfish development.[28,29]

Understanding the crucial role of retinoids and RxR in *A. aurita* development requires insight into the broader context of retinoid signaling. Retinoids are essential for various physiological processes in multicellular organisms, including growth, vision, immune function, and cellular differentiation.[30–35] The active form of vitamin A, 9-cis retinoic acid (RA), serves as a signaling molecule that regulates gene expression and influences cell fate decisions during development.[36] Vitamin A derivatives and

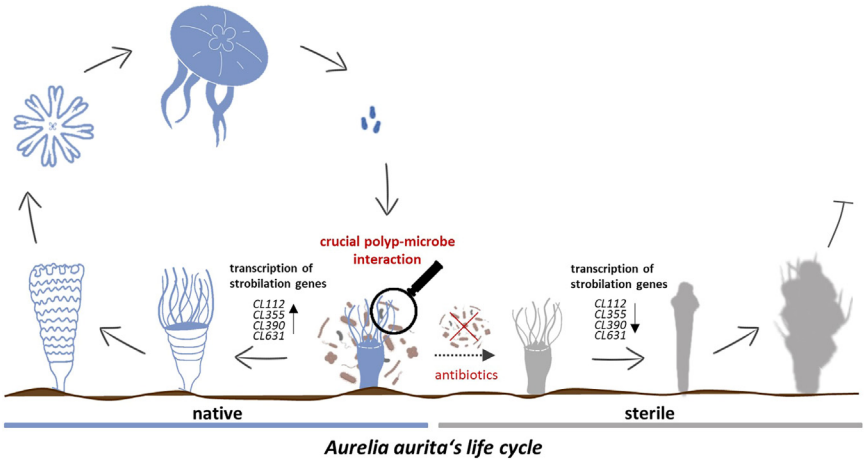

Figure 1. The role of the microbiome in the life cycle of *Aurelia aurita*

A. aurita alternates between the pelagic medusae and the benthic polyp stages. The native microbiome plays a crucial role in the strobilation process, known as strobilation, by activating strobilation genes. In the absence of the native microbiome (sterile conditions), phenotypical abnormalities occur, and strobilation genes are downregulated.

provitamin A from dietary sources are converted into their active form within the multicellular host.[37,38] In this process, retinol undergoes enzymatic oxidation to form all-trans retinal, mediated by retinol dehydrogenase (RDH2), which is then further oxidized to produce 9-cis RA by retinal dehydrogenase (RALDH).[39,40] Once synthesized, 9-cis RA is a potent ligand for nuclear receptors known as retinoic acid receptors (RARs) and RxRs.[41,42] These nuclear receptors function as transcription factors, regulating the expression of target genes involved in various cellular processes, including development, differentiation, and metabolism.[34,43–45] Here, the class of RxR receptors often form heterodimers with other nuclear receptors, including RARs, to modulate the gene expression.[46]

In the context of *A. aurita* development, RxR likely forms a heterodimer with a second receptor upon binding to 9-cis RA.[16] The identity of the second receptor in *A. aurita* remains unknown, although it is known to be activated by an epithelial *CL390* or its analogous biologically active ligand (pharmacophore) 5-methoxy-2-methyl indole (MMI).[16] The heterodimer formed by RxR and its partner receptor binds to specific DNA sequences known as retinoic acid response elements (RAREs) within the regulatory regions of target genes.[41] This binding event impacts the transcription of the target genes (activates or represses), thereby influencing developmental processes such as strobilation.[16] In *A. aurita*, genes such as *CL112*, *CL355*, *CL390*, and *CL631* have been identified to be involved in asexual reproduction.[16,47,48] The transcriptional expression levels of these genes were notably increased when polyps had initiated the strobilation process.[19] This indicated that they have a central role in strobilation and thus they will be cited as strobilation genes in the following. In the absence of native microbiota however, sterile polyps showed a significantly reduced transcription of those strobilation genes compared to polyps with native microbiota, further causing downregulation of general developmental genes (Figure 1).[19]

It is well-established that vitamin A and its derivatives (retinoids) are sourced from the diet in two forms: preformed vitamin A from animal products (retinyl esters, retinol, and small amounts of RA) and provitamin A carotenoids from vegetables and fruits.[49] Among these, beta carotene is the most abundant vitamin A precursor.[50] Bacterial species also possess the enzymatic pathways to generate beta carotene, which can then be absorbed and utilized by the host organism.[51,52] In detail, bacteria utilize pyruvate and D-glyceraldehyde-3-phosphate (GAP) from glycolysis to synthesize isoprenoid precursors via the methylerythritol phosphate (MEP) pathway, also known as the non-mevalonate pathway, resulting in geranylgeranyl diphosphate (GGPP) formation.[53,54] Within the carotenoid biosynthesis pathway two molecules of GGPP condensate to form phytoene, which is then converted into various intermediates through a series of desaturation and isomerization reactions.[53,55] Subsequently, cyclization reactions occur, leading to the formation of carotenoids such as beta carotene, lycopene, lutein, and zeaxanthin.[56] Those carotenoids are absorbed by the host for vitamin A provision.[57] Taking together, we hypothesize that the *Aurelia*-associated microbiome produces beta carotene, which might be as important as dietary sources in contributing to the host's vitamin A supply, emphasizing the metaorganism concept. Such a symbiotic relationship underscores the intricate ecological interactions that contribute to the overall health and well-being of the host. Thus, we hypothesize that the native *A. aurita* polyp microbiome likely plays a pivotal role for offspring generations in supplementing the host's diet with provitamin A carotenoids, particularly beta carotene.

Consequently, we aimed to experimentally decipher the complex interplay between associated bacteria and the host to activate downstream strobilation genes through a RxR heterodimer-based mechanism on the molecular level. Based on different approaches using *A. aurita* polyps from the North Atlantic subpopulation, we achieved strong evidence for the crucial requirement of bacteria-generated provitamin A carotenoids for *A. aurita* offspring generation.

RESULTS

Retinoic acid key genes are induced during strobilation in *A. aurita* and beta carotene dependent

To study the effects of key enzymes of the host RA signaling pathway, the expression of the respective genes encoding beta carotene dioxygenase (BCO1), retinal dehydrogenase (RALDH), and retinol dehydrogenase (RDH2) were studied. Their transcriptional regulation from the polyp stage to the early strobila stage, four days post-strobilation induction with 5-methoxy-2-methyl-indole (MMI), were investigated using qRT-PCR

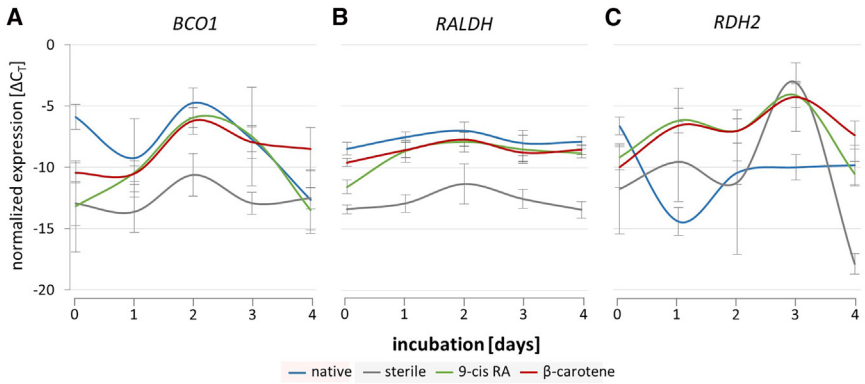

Figure 2. Transcription of retinoic acid signaling genes in *A. aurita* during the onset of strobilation

(A–C) Native and sterile *A. aurita* polyps underwent a three-day incubation with 5 μM 5-methoxy-2-methylindole with daily refreshment, inducing strobilation. Concurrently, 1 μM beta carotene and 100 nM 9-cis retinoic acid (RA) were added to sterile polyps with 5-methoxy-2-methylindole, refreshed daily for 3 days. Gene expression profiles, represented by normalized C_T values (ΔC_T), were analyzed using the housekeeping gene *EF1* for normalization of (**A**) *BCO1*, (**B**) *RALDH,* and (**C**) *RDH2*. C_T values were averaged from three biological replicates, each with three technical replicates (see also Table S1). Data are represented as mean ± SEM.

(Figure 2, Table S1). Expressions in native polyps, sterile control polyps, and sterile polyps supplemented with the active vitamin A metabolite 9-cis RA and provitamin A compound beta carotene was compared. Average cycle thresholds (C_T) values, obtained from three biological replicates with three technical replicates each, were normalized using *EF1* as a reference gene (C_T value of 20.66 ± 1.42) (Table S1).

BCO1 expression in native control polyps peaked at day 2 post-strobilation induction, declining thereafter until the early strobila stage (Figure 2A, blue line). Sterile control polyps exhibited five times lower expression levels but a similar pattern (Figure 2A**,** gray line). Sterile polyps treated with 9-cis RA had similar BCO1 expression to sterile polyps during the polyp stage, but post-strobilation induction levels matched those of native controls (Figure 2A, green line). Sterile polyps supplemented with beta carotene initially showed reduced expression (Figure 2A, red line), later aligning with native polyps and 9-cis RA-treated polyps. RALDH expression exhibited an undulating pattern across all polyp groups, with periodic fluctuations from the polyp to early strobila stages (Figure 2B). In contrast, sterile polyps showed significantly reduced amplitude in these fluctuations (Figure 2B, gray line), indicating an altered expression in the absence of the native microbiome. Both beta carotene and 9-cis RA treatments of sterile polyps displayed similar patterns and levels to native animals, suggesting a restored response (Figure 2B, blue, green, and red lines). RDH2 expression in native control polyps showed biphasic expression, with a decrease in expression after strobilation induction but stabilized again until the early strobila phase (Figure 2C, blue line). Sterile controls and supplemented polyps displayed an oscillatory dynamic with modest regulation during the polyp stage, peaking on the third day post induction before declining during the early strobila stage (Figure 2C, gray, green and red lines). This pattern suggests that RDH2 transcription remains more or less unaffected, which is inline with the prediction that beta carotene is converted to 9-cis RA by BCO and RALDH.

Overall the experiment demonstrates that RA pathway key genes, including BCO1, and RALDH, undergo dynamic regulation during strobilation in *A. aurita*, marking the first characterization of their role in *A. aurita*. Supplementation of sterile polyps with 9-cis RA or beta carotene restores their expression patterns to resemble native conditions in presence of the microbiome.

Strobilation in *A. aurita* requires beta carotene

To unravel the intricate interplay between microbial impact and host signaling pathways in *A. aurita* strobilation (an asexual reproduction), a thorough series of strobilation experiments of *A. aurita* polyps was conducted under selective conditions. The transition from polyp-to-ephyra was monitored by observing strobilae formation and ephyrae release. This investigation aimed to dissect the effects of various host-derived components of the RA pathway compared to most likely bacterial-produced beta carotene on strobilation progression in *A. aurita*.

Initially, strobilation was induced in native and sterile control polyps using MMI. In native polyps, 88% ($N = 48$, Table S2) initiated strobilation, forming early strobilae. By day nine, 86% exhibited full segmentation, developing into late strobilae with an average of eleven segments. Ephyrae release commenced from day twelve, averaging 10 ephyrae per animal (Figures 3A and 3B, native control). In contrast, only 49% of sterile polyps ($N = 47$, Table S2) formed early strobilae, showing morphological abnormalities such as reduced tentacle length, slim body shape, colorless appearance, and delayed segmentation. Sterile late strobilae were shorter, with fewer segments (average of three) and unabsorbed tentacles (Tables S2 and S3, Figures 3A and 3B, sterile control). Ultimately, only 11% of sterile strobilae released ephyrae after twelve days, increasing to 51% by the end of the experiment, with an average of one ephyra per animal (Figures 3A and 3B, sterile control).

Next, both native and sterile polyps were exposed to the strobilation inducer MMI along with 1 μM of retinol without any effect on native polyps concerning segmentation (10 constrictions), early and late strobila formation (88% and 88%, respectively), or ephyra release (75%, ten released ephyrae) compared to native conditions without retinol (Table S2). In sterile polyps however, retinol supplementation led to early strobila formation in 70% of polyps, with an average of eight segments. During strobilation progression, 63% formed late strobilae, with 48% releasing an average of eight ephyrae (Tables S2 and S3, Figures 3A and 3B, retinol). Similarly, presence of 100 nM 9-cis RA per polyp did not affect strobilation characteristics or timing in native polyps (Table S2). Remarkably, in sterile polyps, 9-cis RA fully restored the strobilation process despite the absence of the native microbiome. Early strobilae formed in 84% of polyps, with an average of eleven segments. Late strobilae were formed

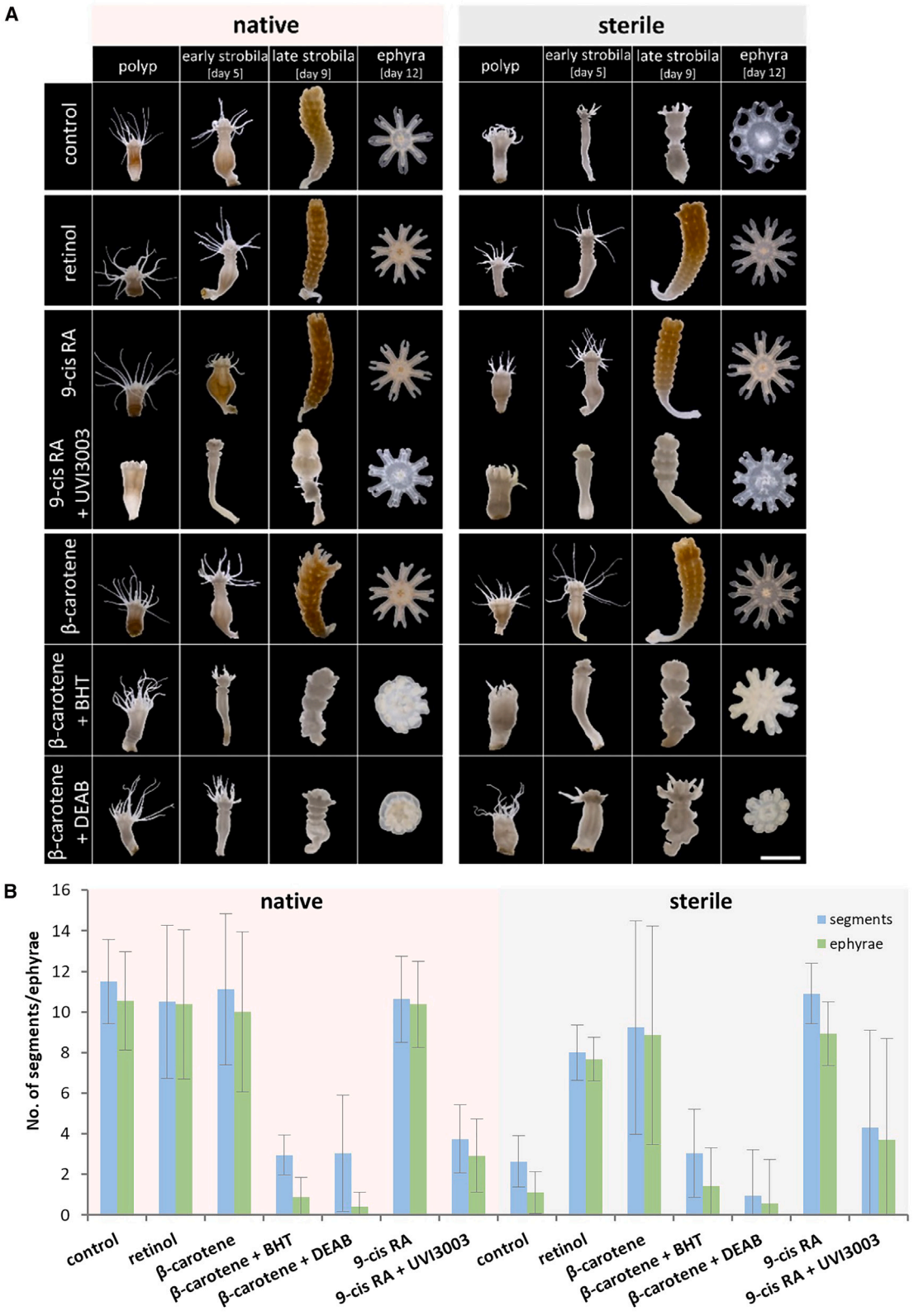

(legend on next page)

by 87% of polyps, with 80% releasing an average of nine ephyrae after twelve days (Tables S2 and S3, Figures 3A and 3B, 9-cis RA), comparable to native control polyps. Moreover, no morphological abnormalities were detected.

The direct impact of 9-cis RA on strobilation was further validated using UVI3003, a selective RxR antagonist, to inhibit its binding to the nuclear receptor RxR. The obtained effects of UVI3003 supplemented in addition to 9-cisRA strongly indicated the binding of 9-cis RA to RxR, underscoring the specific influence of 9-cis RA on the strobilation process (Tables S2 and S3, Figures 3A and 3B, 9-cis RA + UVI3003).

Ultimately, strobilation was induced in native and sterile polyps to test the hypothesis that beta carotene supplementation mimics the presence of a carotene-producing microbiota. Polyps were pre-incubated with 1 μM beta carotene per polyp for 24 h. They were then treated with 5 μM MMI and 1 μM beta carotene per polyp for three days. In native polyps, beta carotene did not affect strobilation, segmentation, or ephyrae release (Tables S2 and S3, Figures 3A and 3B, beta carotene). However, in sterile polyps, beta carotene supplementation led to the formation of 73% early strobilae and 79% late strobilae, with an average of nine segments. Additionally, 98% of these polyps released an average of nine ephyrae, with 51% releasing within 12 days, compared to 69% in native polyps (Tables S2 and S3, Figures 3A and 3B, beta carotene). The life stage phenotypes of β-carotene-supplemented polyps were similar to those of native polyps.

To confirm the role and metabolism of beta carotene in the strobilation of *A. aurita*, polyps were treated with 2,6-Di-*tert*-butyl-4-methylphenol (BHT) to inhibit beta carotene dioxygenase (BCO1), preventing beta carotene conversion to all-trans retinal. In a separate experiment, conversion of all-trans retinal to 9-cis RA was inhibited with dimethylaminobenzaldehyde (DEAB). Both inhibitors caused malformed phenotypes and delayed strobilation in the presence of beta carotene (Tables S2 and S3, Figures 3A and 3B, beta carotene+BHT, beta carotene+DEAB) due to the interfered RA signaling, again underscoring the critical role of beta carotene and 9-cis RA in the strobilation process.

β carotene influences the transcription of strobilation genes in *A. aurita*

Based on the findings regarding the influence of retinoids on the morphological expression of strobilation in *A. aurita*, the impact of 9-cis RA and beta carotene was also investigated at the molecular level, compared to native and sterile control polyps. Expression profiles of the *A. aurita*-specific strobilation genes *CL112*, *CL355*, *CL390*, and *CL631* were analyzed across the developmental stages polyp, early strobila, late strobila, and ephyra in native and sterile control polyps and in sterile polyps supplemented with 9-cis RA or beta carotene (Figure 4). In native control polyps the same expression profile was observed for all strobilation genes (Figure 4, native control). This pattern entailed a gradual increase in expression levels from the initial stages, reaching a peak at the late strobila, and then gradually decreasing toward the medusa stage (Figure 4, native control). These observations aligned with previously documented transcription patterns[19] and corroborated the morphological findings (Figure 3A). Conversely, sterile control polyps exhibited no expression of strobilation genes across all monitored life stages, (Figure 4, sterile control). However, sterile polyps supplemented with 9-cis RA yielded expression profiles similar to those of native controls for strobilation genes, undergoing comparable changes throughout the developmental stages (Figure 4, sterile, 9-cis RA). Similarly, beta carotene led to expression patterns resembling those observed for 9-cis RA and native controls, exhibiting similar normalized C_T values (Figure 4, sterile, beta carotene, Table S1). This expression pattern of strobilation genes clearly verifies the beta carotene's crucial role in strobilation obtained by morphological assessments, in addition at the molecular level.

The associated microbiome provides beta carotene essential for strobilation in *A. aurita*

Since the importance of the RA pathway in the strobilation process of *A. aurita* has been verified, the hypothesis that the microbiome's pivotal role in this process is supplying provitamin A components like beta carotene was further investigated on the microbiome level. Two strategies were employed to validate this hypothesis and elucidate the microbiome's function in facilitating strobilation and offspring generation by providing beta carotene. Firstly, antibiotic treatment was used to reduce microbiota complexity with subsequent correlation of the remaining bacteria with strobilation success. Secondly, genes associated with the bacterial MEP pathway and carotenoid biosynthesis within the native *A. aurita*-associated microbiome were identified and transcription levels elucidated to assess their potential contribution to beta carotene production.

A diverse microbial community is needed for strobilation success

The microbial composition of native polyps analyzed by 16S rRNA amplicon sequencing has been previously reported.[18,19] In this current study the native microbiota composition was confirmed, reflected by the presence of the classes Bacteroidia, γ-Proteobacteria, and α-Proteobacteria, with smaller contributions from other bacterial classes grouped as "Others". Sterile control polyps showed no amplification success during sequencing library preparation, confirming successful removal of associated microbiota. Single-dose antibiotics (Ampicillin, Neomycin,

Figure 3. Restoration of strobilation by beta carotene in sterile *A. aurita* polyps

(A) Strobilation progression of native (left panel) and sterile (right panel) polyps was monitored. The influence of compounds from the retinoic acid signaling pathway and provitamin A component beta carotene on the strobilation process was similarly assessed. The compounds included: 1 μM retinol, 100 nM 9-cis retinoic acid (RA), 100 nM 9-cis RA along with the inhibitor 5 μM UVI3003, 1 μM beta carotene, 1 μM beta carotene along with the antagonist 5 μM 2,6-Di-*tert*-butyl-4-methylphenol (BHT), and 1 μM beta carotene along with the inhibitor 10 μM dimethylaminobenzaldehyde (DEAB). The scale bar, applicable to all images, corresponds to 2 mm.

(B) Daily monitoring of generated strobilae included quantifying segments per strobila 9 days post-induction and monitoring released ephyrae over 24 days. Significances (*p*-values) are detailed in Table S3. Data are represented as mean ± SEM.

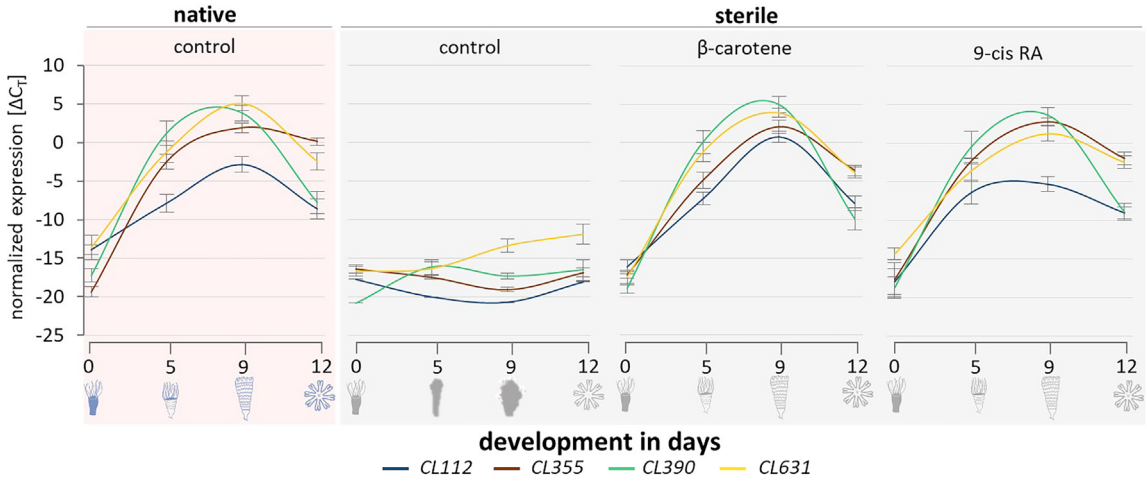

Figure 4. Transcription profiles of strobilation genes during the progression of strobilation under the influence of beta carotene and 9-cis retinoic acid

Transcription profiles of strobilation genes (*CL112*, *CL355*, *CL390*, and *CL631*) were examined in both native and sterile polyps. Sterile polyps were further analyzed with daily supplementation of 1 μM beta carotene and 100 nM 9-cis retinoic acid (RA) over a period of three days. These analyses were conducted during various stages of strobilation (polyp, early and late strobila, ephyra). The gene expression dynamics were depicted using normalized cycle threshold values (ΔC_T), with normalization performed using the housekeeping gene *EF1*. The C_T values represent averages obtained from four biological replicates, each comprising three technical replicates (See also Table S1). Data are represented as mean ± SEM.

Rifampicin) and Provasoli's broad-spectrum antibiotic mixture[18] were used to reduce microbiota in numbers and diversity. After the respective treatment, viable cell counts revealed a significant decrease in colony-forming units (CFU) on MB agar plates. Native control polyps yielded 9100 CFU/polyp, while single-dose antibiotic-treated polyps showed a reduction to 260–286 CFU/polyp. Provasoli's treatment resulted in a further decrease to 68 CFU/polyp (Figure 5A). This reduction was validated by visualizing absolute abundance after 16S amplicon sequencing, showing a significant decrease in sequence reads for Provasoli's treatment, but not for single-dose treatments (Figure 5B). Additionally, amplicon sequencing of single antibiotic-treated polyps showed a relative increase in Bacteroidia, indicating a shift in microbial community composition. In contrast, Provasoli's antibiotic-treated polyps exhibited a dramatic reduction in overall bacterial abundance, especially Bacteroidia (Figure 5B).

Amplicon sequencing observations were correlated with morphological observations throughout the life cycle of *A. aurita*. In native controls, polyps were healthy and well-formed and released 10 medusa. Polyps treated with single antibiotics, Ampicillin, Neomycin, or Rifampicin were similar to native controls but showed effects on segmentation during strobilation (Figure 5C). Ampicillin-treated polyps had clear segmentation, Neomycin-treated polyps had slightly less defined segmentation, and Rifampicin-treated polyps showed the least distinct segmentation. Late strobilae were less robust, especially in Rifampicin-treated polyps. Only four to five segments were formed after single-dose antibiotic treatments compared to twelve in native controls. Ephyra release decreased from eleven in native controls to four in single antibiotic-treated animals (Figure 5D). The released ephyrae were fully formed but less defined, with Neomycin and Rifampicin resulting in the least distinct structures. Under Provasoli's treatment, polyps appeared deformed and less robust. Early strobilae showed less distinct segmentation, and late strobilae had poorly differentiated segments. Ephyrae were less robust and defined compared to native controls. Segmentation and the number of released ephyrae decreased significantly, similar to single-dose antibiotic treatments (Figures 5C and 5D). In summary, while all treatments allowed polyps to reach the ephyra stage, Provasoli's broad-spectrum antibiotic treatment disrupted the normal strobilation process in *A. aurita* polyps by significantly reducing microbial abundance and diversity, highlighting the necessity of an abundant and diverse microbiota for regulating the host RA signaling pathway. This is in agreement with recolonization experiments using single isolates, which all failed to restore the phenotype (data unpublished).

Identification and expression of carotenoid synthesis genes in the microbiome of A. aurita *strongly indicate a bacterial impacted strobilation by β-carotenoids supply*

To obtain further evidence, the presence and expression of bacterial key genes of β-carotenoid synthesis were monitored in the polyp-associated microbiome. Five genes - *dxs*, *ispC*, *ispA*, *crtE*, and *crtI* - known to be involved in the β-carotenoid synthesis were selected (Figure 5E). These gene sequences were searched in bacterial representatives from the NCBI database. Conserved regions for each gene were identified, and degenerated primers were designed. These primers successfully amplified all five genes from DNA extracted from native polyps, while sterile polyps showed no amplification, serving as controls. Consequently, the presence of β-carotenoid synthesis genes for provitamin A compound synthesis were identified exclusively in the native associated microbiota, and not in the host. Sequencing the amplified gene fragments resulted in the identification of *A. aurita* colonizers, all present in the native microbiome (Figure 5B), which are most likely responsible for

A

treatment	CFU/mL
native	9100
Provasolis	68
Ampicillin	286
Neomycin	266
Rifampicin	260

B

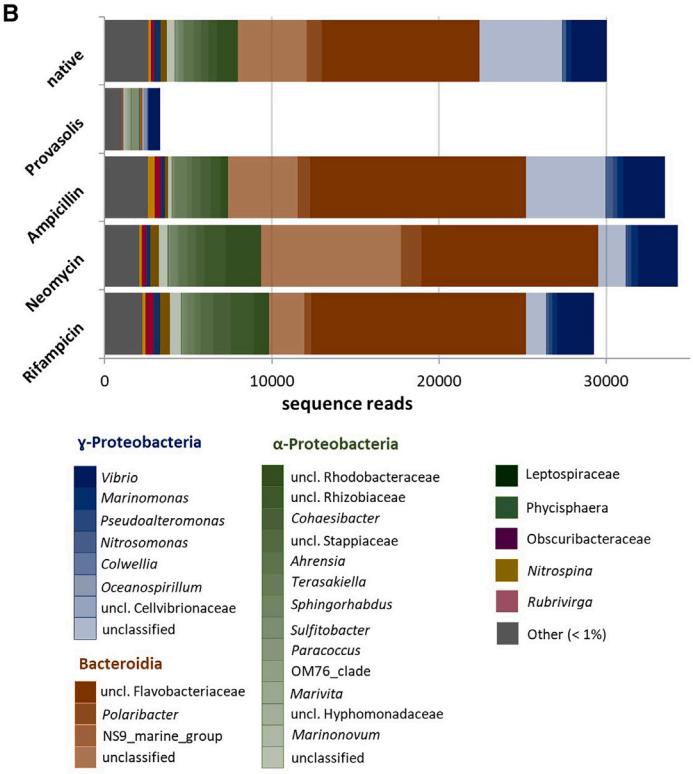

C

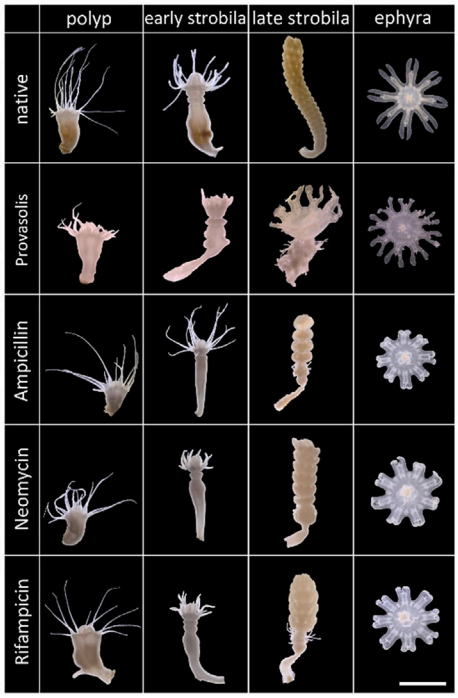

D

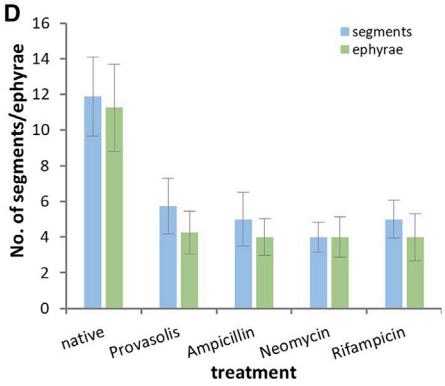

E

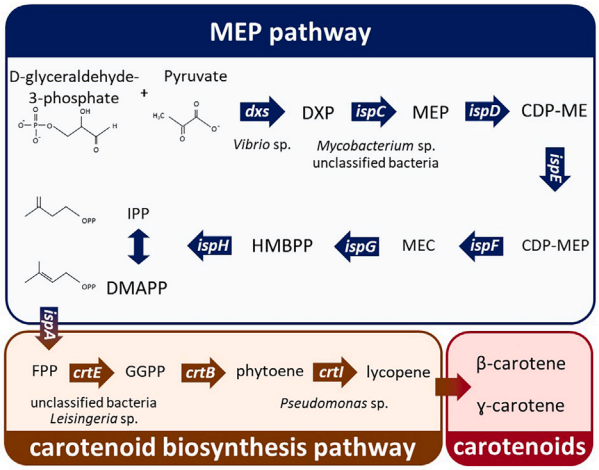

F

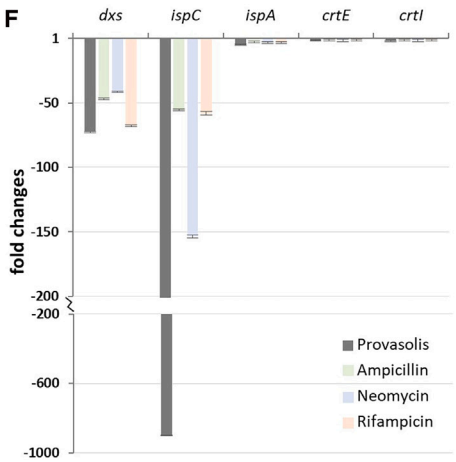

(legend on next page)

providing carotenoids. In more detail, the *dxs* gene was associated with uncultured *Vibrio* sp., *ispC* was linked to *Mycobacterium* sp., unclassified bacteria, *Actinomycetes* sp., *Paraburkholderia* sp., and *Leisingeria* sp. The *crtE* gene was associated with unclassified bacteria, *Mycobacterium* sp., *Leisingeria* sp., *Pleionea* sp., *Caldalkalibacillus* sp., and *Paludibacterium* sp., whereas *crtI* was linked to *Pseudomonas* sp. (Figure 5E, Table S4).

Based on the successful identification of these genes in the native polyp microbiota, the impact of reduced microbiota due to single-dose antibiotics (Ampicillin, Neomycin, Rifampicin) and Provasoli's broad-spectrum antibiotic administration on gene expression was investigated using qRT-PCR. Differential gene expression levels (fold changes) between native and antibiotic-treated polyps showed an overall downregulation in all five genes for all antibiotic-treated animals. Provasoli's treatment significantly reduced the expression levels of all observed genes, indicating a profound disruption in the normal gene expression profile. Single antibiotic treatments had a varied impact, slightly reducing the expression of some genes, indicating a less drastic effect compared to Provasoli's treatment. Specifically, the transcription of *dxs*, the initial gene of the MEP pathway, was 50-fold downregulated in all treatments compared to native control polyps (Figure 5F). This strong downregulation was also observed in *ispC* for the single antibiotic-treated polyps, whereas Provasoli-treated polyps showed even a 900-fold downregulation compared to native controls. For *ispA*, *crtE*, and *crtI*, expression was moderately downregulated by 2- to 5-fold (Figure 5F). These findings emphasize the indispensable role of a diverse and abundant microbiota in facilitating the strobilation process in *A. aurita* most likely by providing provitamin A compounds, with antibiotic treatments disrupting this process by reducing microbial diversity and abundance.

DISCUSSION

In this study, the essential role of the native microbiome in *A. aurita* asexual offspring generation through strobilation was uncovered on the molecular and mechanistic level. The transition from polyp-to-ephyra was monitored by observing strobilae formation and ephyrae release as well as by elucidating the expression of so-called strobilation genes (*CL112, CL355, CL390, and CL631*). The morphological effects of supplementing sterile polyps with bacteria-produced beta carotene were compared to supplementing downstream vitamin A metabolites of the host RA signaling pathway. Molecular consequences were assessed through expression analysis of strobilation-specific host genes by qRT-PCR. Ultimately, the presence and expression of bacterial β-carotenoid synthesis genes were analyzed in the native polyp microbiome compared to antibiotic-treated polyps, demonstrating the microbiome's pivotal role in beta carotene provision. Concluding, we propose that the microbiome-mediated strobilation process of *A. aurita*, is based on the impact of bacterial produced beta carotene on the host RA signaling pathway, which in turn modulated strobilation by activating specific genes through RxR (Figure 6).

The experimental results comprehensively confirmed the model proposed in Figure 6, which hypothesized that beta carotene, synthesized by associated bacteria, serves as a pre-modulator of strobilation in *A. aurita*. Initial morphological observations clearly demonstrated that external supplementation of beta carotene to sterile polyps effectively restored morphological abnormalities induced the absence of a microbiota, validating the pivotal role of microbial-derived compounds in developmental processes (Figures 3 and 4). These findings substantiate the hypothesis that beta carotene, originating from a diverse associated microbiota (Figure 5), plays a central role in RA synthesis within *A. aurita*, illuminating the intricate interplay between microbial and eukaryotic factors in its reproductive cycles. Moreover, these findings emphasize that the abnormalities in the sterile life cycle are not caused by antibiotic treatment but solely by the consequential absence of microbes and their generated beta carotene. In a second line of evidence, the enzymatic pathway in bacteria, involving the condensation of pyruvate and glyceraldehyde 3-phosphate to form DXP and subsequent enzymatic reactions yielding IPP and DMAPP, was confirmed through detecting the presence and expression of key genes of the MEP pathway and carotenoid synthesis in the associated microbiota (Figure 5). The taxonomic classification of bacteria associated with genes involved in the MEP pathway and carotenoid synthesis in *A. aurita* (Table S4), revealed significant ecological and functional implications. Particularly, *Mycobacterium* sp. was consistently associated with both the *ispC* and *crtE* genes, indicating a dual role in the MEP pathway and carotenoid synthesis, contributing to both isoprenoid and carotenoid biosynthesis, which are crucial for strobilation. Unclassified bacteria were also shown to exhibit *ispC* and *crtE* genes, suggesting that poorly understood or undiscovered bacteria likely contributed to these pathways. A higher number of ASVs associated with the *ispC* gene was observed, highlighting its central role in the microbial

Figure 5. Reduction of native microbiota diversity affected strobilation

Fasted, single native polyps were treated with Ampicillin, Neomycin, Rifampicin, or Provasoli's antibiotic mixture.

(A) Colony forming unit (CFU) counts per polyp generated from native and antibiotic-treated polyps were detected after 24 h at 30°C.

(B) Antibiotic-induced changes in bacterial community abundance and diversity were analyzed by 16S rRNA amplicon sequencing. Bar plots show community structure at the genus level as absolute abundances in sequence reads, averaging six replicates per treatment. Taxa with an absolute abundance of <1% are reported as "Other".

(C) Morphology of polyps undergoing strobilation under various conditions, including native polyps and those treated with antibiotics, was examined. Photographs display the phenotypical appearance of polyps, early strobilae, late strobilae, and ephyrae (left to right). The scale bar for all images is 2 mm.

(D) Monitoring of segment generation per strobila for 9 days post-induction, and ephyrae release over 24 days in native and antibiotic-treated polyps.

(E) Bacterial MEP and carotenoid pathways and involved enzymes and their respective genes.

(F) Relative transcript levels of genes involved in the MEP pathway (*dxs*, *ispC*, and *ispA*) and carotenoid biosynthesis (*crtE* and *crtI*) were analyzed in *A. aurita* native control polyps and antibiotic-treated counterparts using qRT-PCR. The analysis included at least three independent biological replicates, each with three technical replicates (see also Table S5). Data are represented as mean ± SEM.

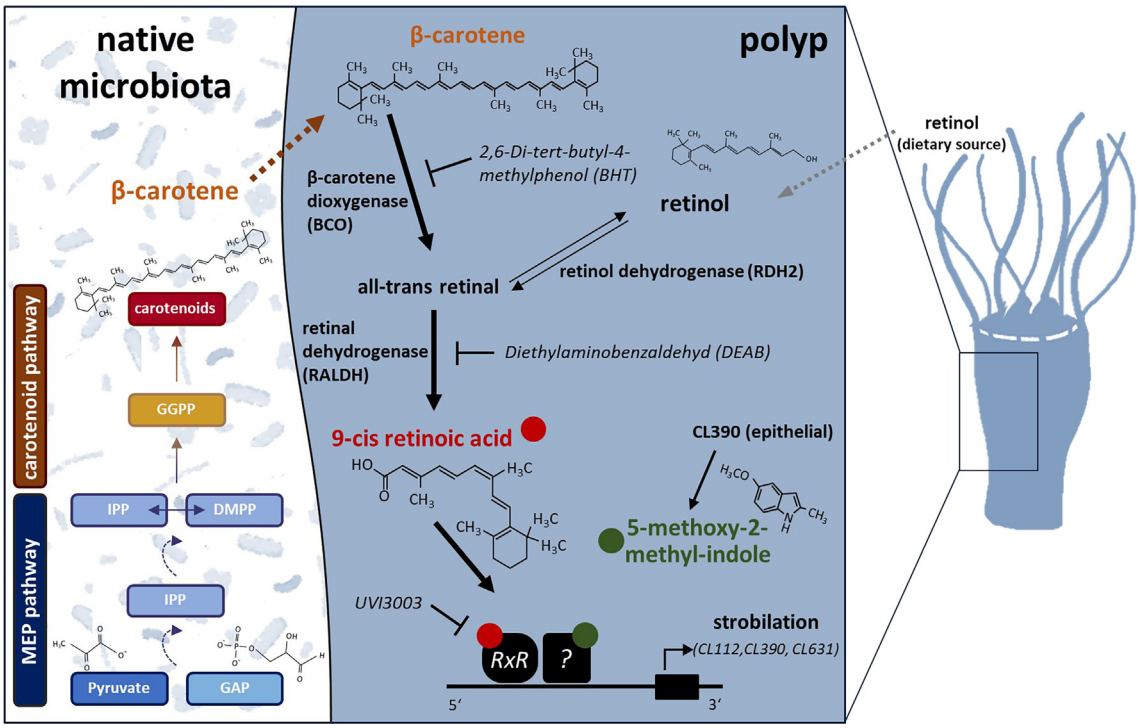

Figure 6. Model of the microbial impact on strobilation in *Aurelia aurita*

Microbial-produced beta carotene, synthesized via the 2-C-methyl-D-erythrol 4-phosphate (MEP) and carotenoid pathways, is hypothesized to present a pre-modulator of strobilation in *A. aurita*. In bacteria, pyruvate and glyceraldehyde 3-phosphate condense to form 1-deoxy-D-xylulose 5-phosphate (DXP), which undergoes enzymatic reactions to yield isopentenyl pyrophosphate (IPP) and dimethylallyl pyrophosphate (DMAPP). Geranylgeranyl pyrophosphate (GGPP), a precursor in isoprenoid biosynthesis, is produced in the carotenoid pathway through the condensation of IPP and DMAPP, subsequently forming beta carotene. Upon cellular uptake, beta carotene undergoes enzymatic cleavages in the polyp host. beta carotene dioxygenase1 (BCO1), antagonized by BHT, catalyzes all-trans retinal production. All-trans retinal is further yielded through reversible isomerization (e.g., retinol dehydrogenase 2). Subsequent oxidation through retinal dehydrogenase (RALDH), inhibited by DEAB, forms 9-cis retinoic acid. This acid serves as a ligand for nuclear receptors, including RxR (inhibited by UVI3003). Upon binding of 9-cis retinoic acid RxR forms a heterodimer with another nuclear receptor, likely activated by 5-methoxy-2-methyl indole. This heterodimer modulates the gene expression of strobilation genes, proposing a microbial-driven pathway where beta carotene, derived from bacteria, plays a crucial role in retinoic acid synthesis, emphasizing the intricate interplay between microbial and eukaryotic factors in the reproductive processes of *A. aurita*.

community's metabolic activities. This finding suggests that the *ispC* gene is critical for the biosynthesis of isoprenoids, which is essential for the host organism. Conversely, the *crtI* gene was found to be associated with a single ASV from *Pseudomonas* sp., indicating that this bacterium might have fulfilled a specialized or niche role in carotenoid synthesis. The diversity of taxa across these genes indicates a complex microbial ecosystem with various functional capabilities, highlighting the importance of microbial interactions in host processes such as strobilation in *A. aurita*. Future studies, e.g., the isolation of representatives of those identified bacterial taxa might clarify which exact bacteria are involved in contributing in carotenoid biosynthesis. Moreover, recolonization experiments with those isolates and genetically manipulated derivatives might allow identifying in detail which component(s) they are contributing and potentially how they interact with the host.

Gene expression analyses on host RA production and subsequent signaling strongly supported these findings, revealing elevated levels of BCO1 and RALDH in native controls and sterile polyps supplemented with beta carotene, in contrast to very low expression levels in sterile polyps (Figure 2). This highlights not only the microbiome's influence on the transcription of key genes in the host RA pathway crucial for strobilation but also represents the first identification of these key genes in *A. aurita*. Furthermore, transcriptional analyses demonstrated that beta carotene significantly influences the expression of strobilation genes across developmental stages in both native and supplemented polyps (Figure 5), strongly indicating that microbiota-derived beta carotene is required for strobilation in *A. aurita* via host RA signaling.

This discovery significantly enhances the mechanistic and molecular understanding of the microbial control mechanisms of the strobilation in *A. aurita*. Given that *A. aurita* plays a fundamental role in marine ecosystems globally, particularly during jellyfish blooms,[58] understanding the complex life cycle of *A. aurita*, especially the strobilation process on the molecular level, is crucial. Jellyfish blooms can significantly impact local ecosystems, fish populations, food webs, and human activities such as fishing and tourism.[17,58–60] Consequently, comprehending the strobilation process is key to managing these blooms and mitigating their effects on marine environments and human industries.[61]

Moreover, the findings from our study on *A. aurita* contribute to a growing body of evidence underscoring the essential roles of microbial symbionts and their metabolites in host developmental processes across a wide range of model organisms.[62,63] Numerous studies have been conducted on various taxa, from Cnidarians to vertebrates, highlighting the intricate and conserved nature of host-microbiome interactions.[64–66] In the Cnidarian *Hydra*, research has demonstrated that its associated microbiota is crucial for normal development and homeostasis.[67] For instance, specific bacterial strains are necessary for the proper development of the epithelial surface.[68,69] Within the invertebrates, the nematode *C. elegans* has been extensively studied, with bacteria-derived folate influencing germline stem cell proliferation.[70] Similarly, in the insect *Drosophila melanogaster*, the gut microbiota impacts host development and metabolism, with gut bacteria affecting insulin signaling and, consequently, growth and development.[71] Among vertebrates, the zebrafish model has provided significant insights into host-microbiome interactions, demonstrating that gut microbiota is essential for normal intestinal development and function in zebrafish.[72] In mammals, particularly mice, the role of gut microbiota has been extensively studied, revealing its influence on various aspects of host development, immunity, and metabolism. A landmark study by Bäckhed et al. (2004)[73] showed that gut microbiota impacts the host's energy storage and fat deposition, highlighting the complex interactions between microbial communities and host physiology. Across these diverse studies, several key trends and mechanisms have emerged. Microbial-produced metabolites, such as short-chain fatty acids, vitamins, and carotenoids, play significant roles in modulating host signaling pathways.[74–76] The microbiota also influences the host's immune system development and function, often by shaping the gut-associated lymphoid tissue.[77] Additionally, microbiota affects various developmental signaling pathways, such as insulin signaling in *Drosophila*.[78]

During the writing process of this paper, Peng et al. (2023)[79] published a study on *Aurelia coerulea* that highlighted microbiota-mediated host phenotype dynamics during strobilation in the jellyfish *A. coerulea* via antibiotic-induced microbiome alteration. They demonstrated that microbial depletion delayed strobilation and reduced segment and ephyra numbers, clearly illustrating the microbiota's influence on development in another species of *Aurelia*.[79] Moreover, metatranscriptome analysis of antibiotic-depleted versus native polyps using the KEGG database pointed to a potential bacterial role in the retinol pathway. Based on their findings, the authors predict that the microbiota regulates the retinal synthesis, and hence affect the production of downstream signaling metabolites, but not directly the RA cascade. PICRUSt2 analysis of 16S rRNA gene sequences revealed the functional potential of associated unclassified Cyanobacteria to promote the expression of RA signaling metabolites before the beginning of strobilation.[79] Our study on *A. aurita* now conclusively complements these findings by experimentally demonstrating with several lines of evidence for the first time, that microbial-derived beta carotene most likely serves as a pre-modulator of strobilation via RA synthesis and gene expression in *A. aurelia*. This discovery underscores the detailed molecular mechanisms and intricate microbial-eukaryotic interactions specific to our model. While Peng et al. focused on broader life cycle transitions and nematocyte dynamics in *A. coerulea*,[79] our research provides a detailed pathway analysis based on experimental data, emphasizing the complementary nature of both studies in understanding microbial influences on *Aurelia* life cycles. In a related context, the findings of Ohdera et al. on *Cassiopea xamachana* further highlight the role of endosymbiont carotenoids in developmental processes, supporting the broader significance of carotenoid-driven metamorphosis across different cnidarian species.[80] Typically, plants are recognized as primary sources of carotenoids.[81] However, in recent years, there has been increasing recognition of bacterially produced carotenoids in the study of host-microbe interactions, especially through the identification of endosymbiotic bacteria as significant carotenoid contributors.[82,83]

Importantly, many of these host-microbe interactions are evolutionarily conserved, indicating that microbiota have long played a critical role in the development and physiology of diverse organisms.[84,85] Our findings in *A. aurita*, which demonstrate the central role of bacteria-derived beta carotene in RA synthesis and strobilation, align with these broader trends. This study not only advances our understanding of the microbial molecular control mechanisms underlying strobilation in *A. aurita* but also underscores the evolutionary significance of host-microbiome interactions. These insights can pave the way for further research into developmental biology and potential biotechnological or medical applications, emphasizing the ancient and complex relationship between hosts and their microbiota.

Conclusion

In conclusion, this study offers significant mechanistic and molecular insights into the microbiota-mediated regulation of strobilation in *A. aurita*, simultaneously opening several new avenues for further investigations and generating new questions. One example is to elucidate, whether the underlying mechanism of beta carotene transfer from microbiota to the host is an active or passive transfer. Various mechanisms for β-carotenoid export from bacteria to host organisms have been proposed.[86,87] These include passive diffusion through the bacterial cell membrane, facilitated transport by specialized proteins like efflux pumps or specific carriers, and transport via outer membrane vesicles (OMVs) that fuse with host cell membranes.[88,89] Additionally, β-carotenoids may be released upon bacterial cell lysis, influenced by environmental stressors.[90] However, the exact mechanisms of carotenoid transfer remain unclear.[91] Preliminary experiments from our group suggest that direct contacts between polyps and the microbiota is crucial for regular reproductive output, possibly mediated through mucus interaction.[19] Understanding these transfer mechanisms will not only shed light on bacterial environmental (host) interactions but will also allow identifying strategies to enhance the bioavailability and health benefits of bacterial β-carotenoids for hosts.

A second avenue for investigation involves exploring the temporal dynamics of microbiome changes and their immediate effects on strobilation, which could clarify causal relationships. Metagenomic approaches to identify specific microbial species or strains responsible for beta carotene production might provide additional mechanistic insights. Finally, studying how these

findings translate to natural environments, with their complex microbial diversity, would be insightful. Assessing the long-term effects of microbiota disruption on jellyfish growth, survival, and subsequent generations could reveal broader ecological implications. Additionally, exploring alternative sources or mechanisms of RA pathway activation beyond beta carotene may uncover additional regulatory pathways in *A. aurita* strobilation. These research avenues underscore the need for continued investigation into the intricate interactions between microbiota and hosts in marine environments, promising deeper insights into developmental processes and ecosystem dynamics.

Ultimately, understanding how microbes facilitate crucial developmental processes in hosts could lead to innovative strategies for managing jellyfish blooms and mitigating their impact on marine ecosystems.

Limitations of the study

While this study provides valuable insights into the role of microbiota-derived beta carotene in the strobilation process of *Aurelia aurita*, there are two limitations that should be acknowledged. First, although we demonstrated the restoration of strobilation through the addition of beta carotene on morphological and molecular level, we did not determine the precise concentration of beta carotene. Furthermore, while we focused on four key genes reported to be associated with strobilation, knockout experiments to directly assess their functional roles in strobilation were not performed due to a missing genetic system. Future studies incorporating those aspects will further strengthen the mechanistic understanding of how beta carotene and RA signaling influence strobilation.

RESOURCE AVAILABILITY

Lead contact

Further information and requests for resources and reagents should be directed to and will be fulfilled by the lead contact, Ruth Anne Schmitz (rschmitz@ifam.uni-kiel.de).

Materials availability

This study did not generate unique reagents.

Data and code availability

- 16S rRNA gene sequencing data has been deposited at the NCBI database and is publicly available as of the date of publication. Accession numbers are listed in the key resources table and are available within the Bioproject PRJNA1125839. The gene sequencing data is available under https://zenodo.org/records/13284011.
- This paper does not report original code.
- Any additional information required to reanalyze the data reported in this paper is available from the lead contact upon request.

ACKNOWLEDGMENTS

This work was conducted with the financial support of the DFG, Germany, as part of the CRC1182 "Origin and function of metaorganisms" (Project B2, Schmitz-Streit and project Z2). We thank Nicole Pinnow for experimental support. We thank the staff of the IKMB (Kiel) sequencing facilities and Sven Künzel and colleagues from the Department for Evolutionary Genetics of the Max Planck Institute for Evolutionary Biology for performing Illumina sequencing.

AUTHOR CONTRIBUTIONS

N.J., N.W.-B. and R.A.S. designed the research; N.J. performed the research; C.M.C. analyzed the sequence data; N.J., N.W.-B., and R.A.S. wrote the paper; N.J., N.W.-B., and R.A.S. edited the paper.

DECLARATION OF INTERESTS

The authors declare no competing interests.

STAR★METHODS

Detailed methods are provided in the online version of this paper and include the following:

- KEY RESOURCES TABLE
- EXPERIMENTAL MODEL AND STUDY PARTICIPANT DETAILS
  - Animal use of Aurelia aurita polyps
  - Generation of germ-free polyps
- METHOD DETAILS
  - Strobilation induction
  - Inhibition of BCO1, RALDH, and RxR
  - Gene expression analysis
  - Total RNA isolation and cDNA synthesis
  - qRT-PCR analysis
  - Reduction of the *A. aurita*-associated microbiota
  - Bacterial MEP and carotenoid synthesis
- QUANTIFICATION AND STATISTICAL ANALYSIS

SUPPLEMENTAL INFORMATION

Supplemental information can be found online at https://doi.org/10.1016/j.isci.2024.111729.

Received: September 12, 2024
Revised: November 4, 2024
Accepted: December 30, 2024
Published: January 2, 2025

REFERENCES

1. Bosch, T.C., and McFall-Ngai, M.J. (2011). Metaorganisms as the new frontier. Zoology (Jena) *114*, 185–190. https://doi.org/10.1016/j.zool.2011.04.001.
2. McFall-Ngai, M., Hadfield, M.G., Bosch, T.C., Carey, H.V., Domazet-Lošo, T., Douglas, A.E., Dubilier, N., Eberl, G., Fukami, T., Gilbert, S.F., et al. (2013). Animals in a bacterial world, a new imperative for the life sciences. Proc. Natl. Acad. Sci. USA *110*, 3229–3236. https://doi.org/10.1073/pnas.1218525110.
3. Bordenstein, S.R., and Theis, K.R. (2015). Host Biology in Light of the Microbiome: Ten Principles of Holobionts and Hologenomes. PLoS Biol. *13*, e1002226. https://doi.org/10.1371/journal.pbio.1002226.
4. Collins, S.M., Surette, M., and Bercik, P. (2012). The interplay between the intestinal microbiota and the brain. Nat. Rev. Microbiol. *10*, 735–742. https://doi.org/10.1038/nrmicro2876.
5. Sommer, F., and Bäckhed, F. (2013). The gut microbiota–masters of host development and physiology. Nat. Rev. Microbiol. *11*, 227–238. https://doi.org/10.1038/nrmicro2974.
6. Gilbert, S.F., Bosch, T.C., and Ledón-Rettig, C. (2015). Eco-Evo-Devo: developmental symbiosis and developmental plasticity as evolutionary agents. Nat. Rev. Genet. *16*, 611–622. https://doi.org/10.1038/nrg3982.
7. Esser, D., Lange, J., Marinos, G., Sieber, M., Best, L., Prasse, D., Bathia, J., Rühlemann, M.C., Boersch, K., Jaspers, C., and Sommer, F. (2019). Functions of the Microbiota for the Physiology of Animal Metaorganisms. J. Innate Immun. *11*, 393–404. https://doi.org/10.1159/000495115.

8. Delzenne, N.M., Knudsen, C., Beaumont, M., Rodriguez, J., Neyrinck, A.M., and Bindels, L.B. (2019). Contribution of the gut microbiota to the regulation of host metabolism and energy balance: a focus on the gut-liver axis. Proc. Nutr. Soc. *78*, 319–328. https://doi.org/10.1017/s0029665118002756.

9. Moitinho-Silva, L., Díez-Vives, C., Batani, G., Esteves, A.I., Jahn, M.T., and Thomas, T. (2017). Integrated metabolism in sponge-microbe symbiosis revealed by genome-centered metatranscriptomics. ISME J *11*, 1651–1666. https://doi.org/10.1038/ismej.2017.25.

10. Weiland-Bräuer, N., Koutsouveli, V., Langfeldt, D., and Schmitz, R.A. (2023). First insights into the Aurelia aurita transcriptome response upon manipulation of its microbiome. Front. Microbiol. *14*, 1183627. https://doi.org/10.3389/fmicb.2023.1183627.

11. Hussain, T., Wang, J., Murtaza, G., Metwally, E., Yang, H., Kalhoro, M.S., Kalhoro, D.H., Rahu, B.A., Tan, B., Sahito, R.G.A., et al. (2021). The Role of Polyphenols in Regulation of Heat Shock Proteins and Gut Microbiota in Weaning Stress. Oxid. Med. Cell. Longev. *2021*, 6676444. https://doi.org/10.1155/2021/6676444.

12. Wang, Y., and Xie, Z. (2022). Exploring the role of gut microbiome in male reproduction. Andrology *10*, 441–450. https://doi.org/10.1111/andr.13143.

13. Lucas, C.H., Graham, W.M., and Widmer, C. (2012). Jellyfish life histories: role of polyps in forming and maintaining scyphomedusa populations. Adv. Mar. Biol. *63*, 133–196. https://doi.org/10.1016/b978-0-12-394282-1.00003-x.

14. Weiland-Bräuer, N., Neulinger, S.C., Pinnow, N., Künzel, S., Baines, J.F., and Schmitz, R.A. (2015). Composition of Bacterial Communities Associated with Aurelia aurita Changes with Compartment, Life Stage, and Population. Appl. Environ. Microbiol. *81*, 6038–6052. https://doi.org/10.1128/aem.01601-15.

15. Spangenberg, D.B. (1965). A study of strobilation in Aurelia aurita under controlled conditions. J. Exp. Zool. *160*, 1–9.

16. Fuchs, B., Wang, W., Graspeuntner, S., Li, Y., Insua, S., Herbst, E.M., Dirksen, P., Böhm, A.M., Hemmrich, G., Sommer, F., et al. (2014). Regulation of polyp-to-jellyfish transition in Aurelia aurita. Curr. Biol. *24*, 263–273. https://doi.org/10.1016/j.cub.2013.12.003.

17. Goldstein, J., and Steiner, U.K. (2020). Ecological drivers of jellyfish blooms - The complex life history of a 'well-known' medusa (Aurelia aurita). J. Anim. Ecol. *89*, 910–920. https://doi.org/10.1111/1365-2656.13147.

18. Weiland-Bräuer, N., Pinnow, N., Langfeldt, D., Roik, A., Güllert, S., Chibani, C.M., Reusch, T.B.H., and Schmitz, R.A. (2020). The Native Microbiome is Crucial for Offspring Generation and Fitness of Aurelia aurita. mBio *11*, e02336-20. https://doi.org/10.1128/mBio.02336-20.

19. Jensen, N., Weiland-Bräuer, N., Joel, S., Chibani, C.M., and Schmitz, R.A. (2023). The Life Cycle of Aurelia aurita Depends on the Presence of a Microbiome in Polyps Prior to Onset of Strobilation. Microbiol. Spectr. *11*, e0026223. https://doi.org/10.1128/spectrum.00262-23.

20. Rewitz, K.F., Yamanaka, N., Gilbert, L.I., and O'Connor, M.B. (2009). The insect neuropeptide PTTH activates receptor tyrosine kinase torso to initiate metamorphosis. Science *326*, 1403–1405. https://doi.org/10.1126/science.1176450.

21. Song, J., and Zhou, S. (2020). Post-transcriptional regulation of insect metamorphosis and oogenesis. Cell. Mol. Life Sci. *77*, 1893–1909. https://doi.org/10.1007/s00018-019-03361-5.

22. Brown, D.D., Wang, Z., Kanamori, A., Eliceiri, B., Furlow, J.D., and Schwartzman, R. (1995). Amphibian metamorphosis: a complex program of gene expression changes controlled by the thyroid hormone. Recent Prog. Horm. Res. *50*, 309–315. https://doi.org/10.1016/b978-0-12-571150-0.50018-4.

23. Denver, R.J. (2013). Neuroendocrinology of amphibian metamorphosis. Curr. Top. Dev. Biol. *103*, 195–227. https://doi.org/10.1016/b978-0-12-385979-2.00007-1.

24. Kayukawa, T., Jouraku, A., Ito, Y., and Shinoda, T. (2017). Molecular mechanism underlying juvenile hormone-mediated repression of precocious larval-adult metamorphosis. Proc. Natl. Acad. Sci. USA *114*, 1057–1062. https://doi.org/10.1073/pnas.1615423114.

25. Niwa, Y.S., and Niwa, R. (2016). Transcriptional regulation of insect steroid hormone biosynthesis and its role in controlling timing of molting and metamorphosis. Dev. Growth Differ. *58*, 94–105. https://doi.org/10.1111/dgd.12248.

26. Mengeling, B.J., Goodson, M.L., and Furlow, J.D. (2018). RXR Ligands Modulate Thyroid Hormone Signaling Competence in Young Xenopus laevis Tadpoles. Endocrinology *159*, 2576–2595. https://doi.org/10.1210/en.2018-00172.

27. Tata, J.R. (1993). Gene expression during metamorphosis: an ideal model for post-embryonic development. Bioessays *15*, 239–248. https://doi.org/10.1002/bies.950150404.

28. Müller, W.A. (1984). Retinoids and pattern formation in a hydroid. J. Embryol. Exp. Morphol. *81*, 253–271.

29. Kostrouch, Z., Kostrouchova, M., Love, W., Jannini, E., Piatigorsky, J., and Rall, J.E. (1998). Retinoic acid X receptor in the diploblast, Tripedalia cystophora. Proc. Natl. Acad. Sci. USA *95*, 13442–13447. https://doi.org/10.1073/pnas.95.23.13442.

30. Takahashi, Y.I., Smith, J.E., Winick, M., and Goodman, D.S. (1975). Vitam A deficiency and fetal growth and development in the rat. J. Nutr. *105*, 1299–1310. https://doi.org/10.1093/jn/105.10.1299.

31. Smith, J., and Steinemann, T.L. (2000). Vitamin A deficiency and the eye. Int. Ophthalmol. Clin. *40*, 83–91. https://doi.org/10.1097/00004397-200010000-00007.

32. Semba, R.D. (1998). The role of vitamin A and related retinoids in immune function. Nutr. Rev. *56*, S38–S48. https://doi.org/10.1111/j.1753-4887.1998.tb01643.x.

33. Huang, Z., Liu, Y., Qi, G., Brand, D., and Zheng, S.G. (2018). Role of Vitamin A in the Immune System. J. Clin. Med. *7*, 258. https://doi.org/10.3390/jcm7090258.

34. Gudas, L.J., and Wagner, J.A. (2011). Retinoids regulate stem cell differentiation. J. Cell. Physiol. *226*, 322–330. https://doi.org/10.1002/jcp.22417.

35. Clagett-Dame, M., and Knutson, D. (2011). Vitamin A in reproduction and development. Nutrients *3*, 385–428. https://doi.org/10.3390/nu3040385.

36. Janesick, A., Wu, S.C., and Blumberg, B. (2015). Retinoic acid signaling and neuronal differentiation. Cell. Mol. Life Sci. *72*, 1559–1576. https://doi.org/10.1007/s00018-014-1815-9.

37. Blaner, W.S., Li, Y., Brun, P.J., Yuen, J.J., Lee, S.A., and Clugston, R.D. (2016). Vitamin A Absorption, Storage and Mobilization. Subcell. Biochem. *81*, 95–125. https://doi.org/10.1007/978-94-024-0945-1_4.

38. Carazo, A., Macáková, K., Matoušová, K., Krčmová, L.K., Protti, M., and Mladěnka, P. (2021). Vitamin A Update: Forms, Sources, Kinetics, Detection, Function, Deficiency, Therapeutic Use and Toxicity. Nutrients *13*, 1703. https://doi.org/10.3390/nu13051703.

39. Lidén, M., and Eriksson, U. (2006). Understanding retinol metabolism: structure and function of retinol dehydrogenases. J. Biol. Chem. *281*, 13001–13004. https://doi.org/10.1074/jbc.R500027200.

40. Napoli, J.L. (1996). Retinoic acid biosynthesis and metabolism. FASEB J. *10*, 993–1001. https://doi.org/10.1096/fasebj.10.9.8801182.

41. Dawson, M.I., and Xia, Z. (2012). The retinoid X receptors and their ligands. Biochim. Biophys. Acta *1821*, 21–56. https://doi.org/10.1016/j.bbalip.2011.09.014.

42. Crettaz, M., Baron, A., Siegenthaler, G., and Hunziker, W. (1990). Ligand specificities of recombinant retinoic acid receptors RAR alpha and RAR beta. Biochem. J. *272*, 391–397. https://doi.org/10.1042/bj2720391.

43. Wendling, O., Chambon, P., and Mark, M. (1999). Retinoid X receptors are essential for early mouse development and placentogenesis. Proc. Natl. Acad. Sci. USA *96*, 547–551. https://doi.org/10.1073/pnas.96.2.547.

44. Ahuja, H.S., Szanto, A., Nagy, L., and Davies, P.J. (2003). The retinoid X receptor and its ligands: versatile regulators of metabolic function, cell differentiation and cell death. J. Biol. Regul. Homeost. Agents *17*, 29–45.

45. Huang, J.K., Jarjour, A.A., Nait Oumesmar, B., Kerninon, C., Williams, A., Krezel, W., Kagechika, H., Bauer, J., Zhao, C., Baron-Van Evercooren, A., et al. (2011). Retinoid X receptor gamma signaling accelerates CNS remyelination. Nat. Neurosci. *14*, 45–53. https://doi.org/10.1038/nn.2702.

46. Lefebvre, P., Benomar, Y., and Staels, B. (2010). Retinoid X receptors: common heterodimerization partners with distinct functions. Trends Endocrinol. Metab. *21*, 676–683. https://doi.org/10.1016/j.tem.2010.06.009.

47. Fuchs, B. (2010). Identifikation und funktionelle Analyse von Genen, die den Lebenszyklus von Aurelia aurita kontrollieren. PhD thesis (Kiel University).

48. Wang, W. (2013). Regulation of metamorphosis and the evolution of life cycles: insights from the common moon jelly Aurelia aurita. PhD thesis (Kiel University of Kiel).

49. Booth, S., Johns, T., and Kuhnlein, H. (1992). Natural food sources of vitamin A and provitamin A. Food Nutr. Bull. *14*, 1–15.

50. Miller, A.P., Coronel, J., and Amengual, J. (2020). The role of β-carotene and vitamin A in atherogenesis: Evidences from preclinical and clinical studies. Biochim. Biophys. Acta Mol. Cell Biol. Lipids *1865*, 158635.

51. Rohmer, M., Knani, M., Simonin, P., Sutter, B., and Sahm, H. (1993). Isoprenoid biosynthesis in bacteria: a novel pathway for the early steps leading to isopentenyl diphosphate. Biochem. J. *295*, 517–524. https://doi.org/10.1042/bj2950517.

52. Ye, V.M., and Bhatia, S.K. (2012). Pathway engineering strategies for production of beneficial carotenoids in microbial hosts. Biotechnol. Lett. *34*, 1405–1414. https://doi.org/10.1007/s10529-012-0921-8.

53. Paniagua-Michel, J., Olmos-Soto, J., and Ruiz, M.A. (2012). Pathways of carotenoid biosynthesis in bacteria and microalgae. Methods Mol. Biol. *892*, 1–12. https://doi.org/10.1007/978-1-61779-879-5_1.

54. Banerjee, A., and Sharkey, T.D. (2014). Methylerythritol 4-phosphate (MEP) pathway metabolic regulation. Nat. Prod. Rep. *31*, 1043–1055. https://doi.org/10.1039/c3np70124g.

55. Ram, S., Mitra, M., Shah, F., Tirkey, S.R., and Mishra, S. (2020). Bacteria as an alternate biofactory for carotenoid production: A review of its applications, opportunities and challenges. J. Funct.Foods *67*, 103867.

56. Vachali, P., Bhosale, P., and Bernstein, P.S. (2012). Microbial carotenoids. Methods Mol. Biol. *898*, 41–59. https://doi.org/10.1007/978-1-61779-918-1_2.

57. Kotake-Nara, E., and Nagao, A. (2011). Absorption and metabolism of xanthophylls. Mar. Drugs *9*, 1024–1037. https://doi.org/10.3390/md9061024.

58. Lucas, C.H. (2001). Reproduction and Life History Strategies of the Common Jellyfish, Aurelia Aurita, in Relation to its Ambient Environment (Springer), pp. 229–246.

59. Mills, C.E. (2001). Jellyfish blooms: are populations increasing globally in response to changing ocean conditions? Hydrobiologia *451*, 55–68.

60. Lo, W.-T., Purcell, J.E., Hung, J.-J., Su, H.-M., and Hsu, P.-K. (2008). Enhancement of jellyfish (Aurelia aurita) populations by extensive aquaculture rafts in a coastal lagoon in Taiwan. ICES (Int. Counc. Explor. Sea) J. Mar. Sci. *65*, 453–461.

61. Prieto, L., Astorga, D., Navarro, G., and Ruiz, J. (2010). Environmental control of phase transition and polyp survival of a massive-outbreaker jellyfish. PLoS One *5*, e13793.

62. Klassen, J.L. (2014). Microbial secondary metabolites and their impacts on insect symbioses. Curr. Opin. Insect Sci. *4*, 15–22.

63. Carrier, T.J., and Bosch, T.C. (2022). Symbiosis: the other cells in development. Development *149*, dev200797.

64. McCauley, M., Goulet, T., Jackson, C., and Loesgen, S. (2023). Systematic review of cnidarian microbiomes reveals insights into the structure, specificity, and fidelity of marine associations. Nat. Commun. *14*, 4899.

65. Stévenne, C., Micha, M., Plumier, J.-C., and Roberty, S. (2021). Corals and sponges under the light of the holobiont concept: how microbiomes underpin our understanding of marine ecosystems. Front. Mar. Sci. *8*, 698853.

66. Mallott, E.K., and Amato, K.R. (2021). Host specificity of the gut microbiome. Nat. Rev. Microbiol. *19*, 639–653.

67. Klimovich, A.V., and Bosch, T.C. (2018). Rethinking the role of the nervous system: lessons from the Hydra holobiont. Bioessays *40*, 1800060.

68. Mazmanian, S.K., Liu, C.H., Tzianabos, A.O., and Kasper, D.L. (2005). An immunomodulatory molecule of symbiotic bacteria directs maturation of the host immune system. Cell *122*, 107–118.

69. Fraune, S., and Bosch, T.C. (2010). Why bacteria matter in animal development and evolution. Bioessays *32*, 571–580.

70. MacNeil, L.T., Watson, E., Arda, H.E., Zhu, L.J., and Walhout, A.J. (2013). Diet-induced developmental acceleration independent of TOR and insulin in C. elegans. Cell *153*, 240–252.

71. Shin, S.C., Kim, S.-H., You, H., Kim, B., Kim, A.C., Lee, K.-A., Yoon, J.-H., Ryu, J.-H., and Lee, W.-J. (2011). Drosophila microbiome modulates host developmental and metabolic homeostasis via insulin signaling. Science *334*, 670–674.

72. Rawls, J.F., Samuel, B.S., and Gordon, J.I. (2004). Gnotobiotic zebrafish reveal evolutionarily conserved responses to the gut microbiota. Proc. Natl. Acad. Sci. USA *101*, 4596–4601.

73. Bäckhed, F., Ding, H., Wang, T., Hooper, L.V., Koh, G.Y., Nagy, A., Semenkovich, C.F., and Gordon, J.I. (2004). The gut microbiota as an environmental factor that regulates fat storage. Proc. Natl. Acad. Sci. USA *101*, 15718–15723.

74. Noverr, M.C., and Huffnagle, G.B. (2004). Regulation of Candida albicans morphogenesis by fatty acid metabolites. Infect. Immun. *72*, 6206–6210.

75. Zientz, E., Dandekar, T., and Gross, R. (2004). Metabolic interdependence of obligate intracellular bacteria and their insect hosts. Microbiol. Mol. Biol. Rev. *68*, 745–770.

76. Fraser, P.D., and Bramley, P.M. (2004). The biosynthesis and nutritional uses of carotenoids. Prog. Lipid Res. *43*, 228–265.

77. Rhee, K.-J., Sethupathi, P., Driks, A., Lanning, D.K., and Knight, K.L. (2004). Role of commensal bacteria in development of gut-associated lymphoid tissues and preimmune antibody repertoire. J. Immunol. *172*, 1118–1124.

78. Bernal, A., and Kimbrell, D.A. (2000). Drosophila Thor participates in host immune defense and connects a translational regulator with innate immunity. Proc. Natl. Acad. Sci. USA *97*, 6019–6024.

79. Peng, S., Ye, L., Li, Y., Wang, F., Sun, T., Wang, L., Hao, W., Zhao, J., and Dong, Z. (2023). Microbiota regulates life-cycle transition and nematocyte dynamics in jellyfish. iScience *26*, 108444. https://doi.org/10.1016/j.isci.2023.108444.

80. Ohdera, A.H., Avila-Magaña, V., Sharp, V., Watson, K., McCauley, M., Steinworth, B., Diaz-Almeyda, E.M., Kitchen, S.A., Poole, A.Z., and Bellantuono, A. (2022). Symbiosis-driven development in an early branching metazoan. Preprint at bioRxiv. https://doi.org/10.1101/2022.07.21.500558.

81. Cazzonelli, C.I. (2011). Carotenoids in nature: insights from plants and beyond. Funct. Plant Biol. *38*, 833–847.

82. Pan, X., Raaijmakers, J.M., and Carrión, V.J. (2023). Importance of Bacteroidetes in host–microbe interactions and ecosystem functioning. Trends Microbiol. *31*, 959–971.

83. Sloan, D.B., and Moran, N.A. (2012). Endosymbiotic bacteria as a source of carotenoids in whiteflies. Biol. Lett. *8*, 986–989.

84. Delaux, P.-M., and Schornack, S. (2021). Plant evolution driven by interactions with symbiotic and pathogenic microbes. Science *371*, eaba6605.

85. Tran, H.K.R., Grebenc, D.W., Klein, T.A., and Whitney, J.C. (2021). Bacterial type VII secretion: An important player in host-microbe and microbe-microbe interactions. Mol. Microbiol. *115*, 478–489.

86. Doshi, R., Nguyen, T., and Chang, G. (2013). Transporter-mediated biofuel secretion. Proc. Natl. Acad. Sci. USA *110*, 7642–7647.

87. Rees, D.C., Johnson, E., and Lewinson, O. (2009). ABC transporters: the power to change. Nat. Rev. Mol. Cell Biol. *10*, 218–227.

88. Molnár, J., Gyémánt, N., Mucsi, I., Molnár, A., SZAB, M., Körtvélyesi, T., Varga, A., Molnár, P., and Tóth, G. (2004). Modulation of multidrug resistance and apoptosis of cancer cells by selected carotenoids. In vivo *18*, 237–244.

89. Wang, M., Nie, Y., and Wu, X.L. (2021). Membrane vesicles from a Dietzia bacterium containing multiple cargoes and their roles in iron delivery. Environ. Microbiol. *23*, 1009–1019.

90. López, G.-D., Álvarez-Rivera, G., Carazzone, C., Ibáñez, E., Leidy, C., and Cifuentes, A. (2023). Bacterial carotenoids: extraction, characterization, and applications. Crit. Rev. Anal. Chem. *53*, 1239–1262.

91. Matsushita, Y., Suzuki, R., Nara, E., Yokoyama, A., and Miyashita, K. (2000). Antioxidant activity of polar carotenoids including astaxanthin-β-glucoside from marine bacterium on PC liposomes. Fish. Sci. *66*, 980–985.

92. Kozich, J.J., Westcott, S.L., Baxter, N.T., Highlander, S.K., and Schloss, P.D. (2013). Development of a dual-index sequencing strategy and curation pipeline for analyzing amplicon sequence data on the MiSeq Illumina sequencing platform. Appl. Environ. Microbiol. *79*, 5112–5120. https://doi.org/10.1128/aem.01043-13.

93. Livak, K.J., and Schmittgen, T.D. (2001). Analysis of relative gene expression data using real-time quantitative PCR and the 2(-Delta Delta C(T)) Method. Methods *25*, 402–408. https://doi.org/10.1006/meth.2001.1262.

94. Yilmaz, P., Parfrey, L.W., Yarza, P., Gerken, J., Pruesse, E., Quast, C., Schweer, T., Peplies, J., Ludwig, W., and Glöckner, F.O. (2014). The SILVA and "all-species living tree project (LTP)" taxonomic frameworks. Nucleic Acids Res. *42*, D643–D648.

95. Wood, D.E., Lu, J., and Langmead, B. (2019). Improved metagenomic analysis with Kraken 2. Genome Biol. *20*, 1–13.

96. Lu, J., Breitwieser, F.P., Thielen, P., and Salzberg, S.L. (2017). Bracken: estimating species abundance in metagenomics data. PeerJ Comput. Sci. *3*, e104.

STAR★METHODS

KEY RESOURCES TABLE

REAGENT or RESOURCE	SOURCE	IDENTIFIER
Chemicals, peptides and recombinant proteins, samples		
Ampicillin	Carl Roth	K029.2
Chloramphenicol	Carl Roth	3886.3
Neomycin	Carl Roth	8668.2
Streptomycin	Carl Roth	0236.3
Rifampicin	Carl Roth	4163.2
Spectinomycin	Carl Roth	HP66.2
Penicillin G	Carl Roth	CN28.1
Polymyxin B	Carl Roth	0235.3
Tetracycline	Carl Roth	0237.1
Gentamycin	Carl Roth	0233.3
5-methoxy-2-methyl indole	Merck	M15451
β-carotene	Thermo Fisher Scientific	H60106.06
9-cis retinoic acid	Thermo Fisher Scientific	J62219.LB0
retinol	Thermo Fisher Scientific	J62079.MC
2,6-di-tert-butyl-4-methylphenol	Thermo Fisher Scientific	A16863.30
dimethylaminobenzaldehyde	Thermo Fisher Scientific	X867.1
UVI3003	Merck	SML1950
Critical commercial assays		
WIZARD Genomic DNA purification kit	Promega	A2920
RapidOut DNA Removal Kit	Thermo Fisher Scientific	K2981
SuperScript IV first-strand synthesis kit	Thermo Fisher Scientific	K1612
PCR Clean-up kit	Machery-Nagel	740609.50
Oligonucleotides		
27F 5'-AGAGTTTGATCCTGGCTCAG-3'	Eurofins	N/A
338R 5'-TGCTGCCTCCCGTAGGAGT-3'	Eurofins	N/A
1492R 5'-GGTTACCTTGTTACGACTT-3'	Eurofins	N/A
EF1_F 5'-AGTTCCAGGGGACAATGTTGG-3'	Eurofins	N/A
EF1_R 5'-TGGATTTCGCCAGGATGGTTC-3'	Eurofins	N/A
CL112_F 5'-GAAGCTACCAGATCCGTTTGG-3'	Eurofins	N/A
CL112_R 5'-TGCAAGCGCATCTGTTCACAG-3'	Eurofins	N/A
CL355_F 5'-TTCCGGAGAGCAGACCAATG-3'	Eurofins	N/A
CL355_R 5'-CCAACGGCTGCATATACCATC-3'	Eurofins	N/A
CL390_F 5'-AAGGTGCGACAATGAAGGTCC-3'	Eurofins	N/A
CL390_R 5'-GTCTACAGGCTCAATGGTGTC-3'	Eurofins	N/A
CL631_F 5'-GCCTTGACGGTGAAAGATGAG-3'	Eurofins	N/A
CL631_R 5'-ACCTCGTCCTCATCCTTTTCG-3'	Eurofins	N/A
BCO1_F 5'-GGCCTAAACTACATGCATGACT-3'	Eurofins	N/A
BCO_R 5'-TTGTTGTGCTGTACCGAAGTGAT-3'	Eurofins	N/A
RDH2_F 5'-TCATCTAGAGTCAGCTGCTTGC-3'	Eurofins	N/A
RDH2_R 5'-CCGTCTAGCTTTGTTACTGAGC-3'	Eurofins	N/A
RALDH_F 5'-CCAGCTCTTTGCTGTGG-3'	Eurofins	N/A
RALDH_R 5'-TTTGCCGGCAGCTTGCT-3'	Eurofins	N/A
dxs_F 5'-TCAAARTACCCRACWCTKGC-3'	Eurofins	N/A
dxs_R 5'-CMGTVARRATYTTRTGTGGGTA-3'	Eurofins	N/A

(*Continued on next page*)

Continued

REAGENT or RESOURCE	SOURCE	IDENTIFIER
ispC_F 5'-GGYKCNACNGGHTCDRT-3'	Eurofins	N/A
ispC_R 5'-CNACRATNGCNGCSRT-3'	Eurofins	N/A
ispA_F 5'- CHKSVATGGAYRATGAYG-3'	Eurofins	N/A
ispA_R 5'-TTGNCCVVYRMMCATVC-3'	Eurofins	N/A
crtE_ F 5'-GARMTGRTBCAYKSSG-3'	Eurofins	N/A
crtE_R 5'-AASAGSRYSCYGGTYTT-3'	Eurofins	N/A
crtI_F 5'-TVATYGGBGCVGGHYTK-3'	Eurofins	N/A
crtI_R 5'-ABBBBRTARAASGGVKHVA-3'	Eurofins	N/A
Deposited data		
Raw 16S rRNA gene sequencing data	NCBI	BioProject PRJNA1125839
gene sequencing data	Zenodo	https://zenodo.org/records/13284011
Software and algorithms		
QIIME2 (version qiime2-2021.2)	N/A	N/A
DADA2 pipeline	N/A	N/A
Geneious Prime (version 2020.0.5)	Novartis	N/A

EXPERIMENTAL MODEL AND STUDY PARTICIPANT DETAILS

Animal use of Aurelia aurita polyps

Aurelia aurita polyps (no gender) from the North Atlantic subpopulation (Roscoff, France) were maintained in the laboratory following established protocols.[14,18,19] In brief, polyps were kept in 2 L plastic tanks with artificial seawater (ASW; Tropical Marin Sea Salt, Hobby, Grafschaft-Gelsdorf, Germany) of 30 practical salinity units (PSU) at 19°C with weekly water change. Polyps were fed twice a week with freshly hatched *Artemina salina* (Hobby, Grafschaft-Gelsdorf, Germany).

Generation of germ-free polyps

Generation of germ-free polyps followed an established protocol[19] involving animal fasting at least three days before antibiotic treatment. Sterile polyps were generated by exposing them to an antibiotic mixture for three days, comprising 50 mg/L each of Chloramphenicol, Neomycin, Ampicillin, Streptomycin, and Rifampicin, along with 60 mg/L Spectinomycin in sterile ASW (all antibiotics from Carl Roth, Karlsruhe, Germany). The absence of cultivable bacteria was confirmed by plating the polyp homogenate on Marine Bouillon (MB) and R2A agar plates (Carl Roth, Karlsruhe, Germany) and examining the absence of bacterial colonies after two days of incubation at 30°C. Furthermore, full-length amplification of the 16S rRNA gene was conducted using GoTaq polymerase and the universal primer pair 27F (5'-AGAGTTTGATCCTGGCTCAG-3') and 1492R (5'-GGTTACCTTGTTACGACTT-3'). Genomic DNA isolated from randomly selected antibiotic-treated polyps, extracted using the WIZARD Genomic DNA purification kit (Promega, Madison, WI, USA), served as the template. The lack of amplification verified the observation of sterility. The germ-free life stages early strobila, late strobila, and ephyra were derived from germ-free polyps under sterile keeping conditions during animal development (described above).

METHOD DETAILS

Strobilation induction

Single native and sterile polyps were placed in separate wells of a 48-well plate (Greiner AG, Kremsmünster, Austria), each containing 1 mL of ASW. Strobilation was induced by daily addition of 5 μM 5-methoxy-2-methyl indole per polyp for three days during water exchange (48 replicates per treatment).[18] The initial occurrence of the early strobila stage was identified by the constriction of the first segments at the apical part, marking the onset of the strobilation on day five in native polyps. The segmentation process was completed on day nine for native controls (late strobila). Subsequently, the ephyrae were continuously released from native strobilae from day twelve onwards and their release was monitored until the end of the experiment on day 24. A stereomicroscope (Novex Binoculares RZB-PL Zoom Microscope 65.500, Novex, Arnhem, the Netherlands) equipped with a high-definition multimedia interface camera was utilized for the daily recording of segment development and ephyrae release. Two sample t-test was used to determine the statistical significance between the average numbers of segments and ephyrae per treatment.

Carotenes act as precursors to retinol, which subsequently serves as a precursor to retinoic acid in the metabolic pathway responsible for supplying active vitamin A in animals.[36–38] Stock solutions of β-carotene (1 mM), retinol (1 mM) and 9-cis retinoic acid (100 μM) (all from Thermo Fisher Scientific, Darmstadt, Germany) were prepared in 100 % ethanol and stored at - 20°C. Initially, single

native and sterile polyps were supplemented with 5 μM of 5-methoxy-2-methyl indole per polyp, concurrently with either 1 μM of retinol per polyp/well or 100 nM of 9-cis retinoic acid per polyp/well, aiming to replicate host metabolism for vitamin A. Substances were administered daily for three consecutive days. Final concentrations of retinol and 9-cis RA used in the experiments were determined based on a preliminary experiment involving various concentrations (Figure S1). In a second approach, strobilation induction in single native and sterile polyps was initiated based on the hypothesis that β-carotene supplementation would simulate a carotene-providing microbiota. Therefore, polyps were incubated with 1 μM of β-carotene per polyp for 24 h. Subsequently, polyps were treated with 5 μM of 5-methoxy-2-methyl indole simultaneous to 1 μM of β-carotene per polyp for three days, with daily replacements. Pre-incubation of polyps with 1 μM of β-carotene for 24 h was determined based on a preliminary experiment involving different administration times of β-carotene in relation to 5-methoxy-2-methyl indole induction (Figure S2). Controls consisted of native and sterile polyps receiving exclusive administration of 5-methoxy-2-methyl indole, retinol, 9-cis retinoic acid, or β-carotene, following a similar protocol. Furthermore, both native and sterile polyps were subjected to 0.1 % ethanol exposure for a duration of one week in order to evaluate any potential detrimental impacts of the solvent on the organisms. However, neither the phenotypes nor the survival rates were impacted by the exposure, thus abstaining from the presentation of those evaluation results. Each treatment consisted of 48 replicates and native control groups induced with retinol, 9-cis retinoic acid, or β-carotene implicated 8 replicates.

Inhibition of BCO1, RALDH, and RxR

A series of experiments were conducted to investigate the impact of inhibitors and antagonist on the strobilation process in polyps, each involving 24 native and sterile polyps. In experiment 1, polyps in 1 mL sterile ASW were exposed to a mixture of 5 μM 5-methoxy-2-methyl indole, 1 μM β-carotene, and 1 μM 2,6-di-tert-butyl-4-methylphenol (BHT) for three days. In experiment 2, the polyps were exposed to 5 μM 5-methoxy-2-methyl indole, 1 μM β-carotene, and 10 μM di-ethylaminobenzaldehyde (DEAB) for three days. Experiment 3 involved treatment with 5 μM 5-methoxy-2-methyl indole, 100 nM 9-cis retinoic acid, and 5 μM UVI3003 for three days. Strobilation progression was monitored after the removal of chemicals.

Gene expression analysis

In order to investigate the impact of microbial metabolites, namely β-carotene and 9-cis retinoic acid (RA), on gene expression during the strobilation process in *A. aurita*, qRT-PCR analysis was conducted. In a first experiment, 48 samples were collected and analyzed. These included native polyps, sterile polyps without supplementation, and polyps supplemented with either β-carotene or 9-cis RA. The transcript levels of host key genes involved in the metabolism of these compounds, specifically β-carotene dioxygenase 1 (BCO1), retinaldehyde dehydrogenase (RALDH), and retinoid X receptor (RxR), were assessed. Samples were collected daily over a 4-day period until the emergence of early strobilae. In a second experiment, the analysis was expanded to include different life stages: polyp, early strobila (4 days post-induction), late strobila (9 days post-induction), and ephyra (12 days post-induction). Each stage consisted of 12 replicates, totaling 60 samples. The expression of strobilation-related genes following supplementation with β-carotene or 9-cis RA was investigated.

Total RNA isolation and cDNA synthesis

Individual animals were washed three times with sterile ASW and transferred to 1.5-mL reaction tubes containing 50 μl RNAlater® (Sigma-Aldrich Chemie GmbH, Taufkirchen, Germany). Subsequently, the samples were frozen in liquid nitrogen and stored at -80°C. The frozen animals were homogenized with a motorized pestle (Kontes, DWK Life Science, Wertheim, Germany) resuspended in a 200 μL solution containing 100 nM Tris-HCl (pH 5.5), 10 mM EDTA, 0.1 M NaCL, 1 % SDS, 1 % 2-mercaptoethanol and 2 μL Proteinase K (25 mg/mL; Thermo Fisher Scientific, Darmstadt, Germany). The mixture was incubated for 10 min at 55°C. Protein precipitation was initiated by adding 10 μL of 3 M potassium acetate, followed by treatment with 200 μL ROTI phenol and 70 μL ROTI chloroform / isoamyl alcohol (both from Carl Roth, Karlsruhe, Germany) for 15 min on ice. After a centrifugation step (13,000 rpm for 15 min, 4°C), 200 μL ROTI chloroform / isoamyl alcohol was added to the RNA and centrifuged again under the same conditions. RNA precipitation was performed by adding 1 volume of 2-propanol with a followed centrifugation at 13,000 rpm for 15 min at 4°C. The RNA pellets were washed once with 70 % ice-cold ethanol. Finally, the RNA pellets were dissolved in 40 μL RNase-free water (Carl Roth, Karlsruhe, Germany). According to the manufacturer protocol, DNA contaminations were removed from the RNA samples by DNase treatment with the RapidOut DNA Removal Kit (Thermo Fisher Scientific, Darmstadt, Germany). DNA removal was confirmed by standard PCR analysis with the GoTaq PCR Kit (Promega, Madison, WI, USA; see the manufacturer's protocol) using the 27F and 1492R primers.[92] Following DNA removal, RNA was reverse-transcribed using random hexamers from the SuperScript IV first-strand synthesis kit (Thermo Fisher Scientific, Darmstadt, Germany) according to the manufacturer's instructions. Synthesized cDNA was purified using the PCR Clean-Up Kit (Machery-Nagel, Düren, Germany).

qRT-PCR analysis

Gene expression dynamics in *A. aurita* were analyzed during the strobilation process, focusing on a total of nine genes. Three genes (BCO1, RDH2, and RALDH), associated with the carotenoid/retinoic acid pathway, were analyzed in polyps over a five-day period of incubation with either supplemented β-carotene or 9-cis retinoic acid. The polyps were investigated daily to observe their gene expression dynamics throughout the progression of strobilation. Similarly, strobilation-specific genes *CL112, CL355, CL390, and CL631* were analyzed across the different life stages polyp, early and late strobila, and ephyra in control native and sterile animals

compared to animals supplemented with β-carotene or 9-cis retinoic acid. The housekeeping gene elongation factor 1 (*EF1*) was utilized as a reference for normalization.[16] Reactions were performed in 25 μL using Platinum SYBR green qPCR SuperMix-UDG (Thermo Fisher Scientific, Darmstadt, Germany), incorporating 5 μL of cDNA (20 ng) and 0.4 μM forward and reverse primers, specified in key resources table. Cycle conditions included an initial denaturation step of 50°C for 2 min, followed by 95°C for 2 min, followed by 40 cycles of 95°C for 15 s; 60°C for 30 s; 95°C for 15 s, and 60°C for 30 s, concluding with 95°C for 15 s. Normalization of average cycle thresholds (C_T) values for all samples (four biological with three technical replicates) was performed using *EF1*[16] as a reference, with a C_T maintaining a consistent value of 20.66 ± 1.42. Fold changes in gene regulation were calculated with the $\Delta\Delta C_T$ method.[93]

Reduction of the *A. aurita*-associated microbiota

Before initiating antibiotic treatment, the polyps underwent a fasting period of at least three days. Single native polyps were individually placed in wells of a 48-well plate, each containing 1 mL of sterile ASW. The native polyps were then treated with a dose of Ampicillin, Neomycin, or Rifampicin (each at 50 mg/L; covering different modes of action), dissolved in sterile ASW, or the broad-spectrum Provasoliś antibiotic mixture containing Penicillin G (360.000 U/L), Chloramphenicol (1.5 mg/L), Neomycin (1.8 mg/L), Polymyxin B (9.000 U/L), Tetracycline (15 mg/L), Ampicillin (120 mg/L), Streptomycin (60 mg/L), and Gentamycin (60 mg/L) (all components from Carl Roth, Karlsruhe, Germany), dissolved in sterile ASW. Treatment was administered for three days, with daily replacement of antibiotic mixture. On the fourth day, the antibiotics were washed out three times with sterile ASW before inducing the strobilation process with 5 μM of 5-methoxy-2-methyl indole. The strobilation process was monitored with eight replicates, while eight replicates of native and sterile polyps served as controls. Additionally, twelve native controls and each twelve antibiotic-treated polyps were used for RNA isolation, cDNA synthesis and subsequent qRT PCR analysis to analyze bacterial β-carotene synthesis. For CFU (colony forming units) calculation of native and antibiotic treated polyps, single polyps (3 replicates) were homogenized with a motorized pestle (Kontes, DWK Life Science, Wertheim, Germany) and diluted in 1 mL sterile ASW. The homogenate were plated on MB agar plates and incubated for 24 h at 30°C.

Moreover, further six native, sterile and antibiotic-treated polyps were subjected to DNA isolation following three washing steps with sterile ASW to eliminate transient bacteria. Individual animals were homogenized using a motorized pestle, and total bacterial DNA was extracted using the Wizard Genomic DNA purification kit (Promega, Madison, WI, USA). The 16S rRNA gene primer pair 27F/338R (27 F, 5'-AGAGTTTGATCCTGGCTCAG-3'; 338 R, 5'-TGCTGCCTCCCGTAGGAGT-3') was used in a 25 μL PCR reaction that included 15.3 μL DEPC-water (Roth, Karlsruhe, Germany), 5 μL 5x GoTaq buffer (Promega, Madison, WI, USA), 1 μL 10 μM forward and reverse primers, 2 μL of DNA (20 ng) and 0.2 μL GoTaq® G2 DNA polymerase (Promega, Madison, WI, USA). The PCR program comprised a 3 min pre-denaturation step at 95°C, followed by 29 cycles (95°C for 30 sec, 50°C for 30 sec, and 72°C for 30 sec), and a final 5 min elongation step at 72°C. Samples were used for amplicon sequencing of the bacterial 16S rRNA V1 – V2 region on the MiSeq platform (Illumina) at the Institute for Clinical Molecular Biology, Kiel University.

Paired-end raw read files were processed using QIIME 2 (version qiime2-2021.2). The 16S rRNA gene sequences were denoised using DADA2 via q2-dada2. Quality profile plots were inspected to select values for truncation of forward and reverse reads. The truncation and trimming were set to ""-p-trim-left-f 13, -p-trunc-len –f 250, -p-trunc-len -r 250"". All resulting amplicon sequence variants (ASVs) were aligned with the mafft via q2-align, and this was used to construct a midpoint-rooted phylogeny with fasttree2. The taxonomy for ASV was assigned by aligning ASVs to the SILVA v.138 database.[94] The data were imported into Excel to construct bar plots for bacterial taxonomic assignment. Sequence data was deposited under NCBI BioProject PRJNA1125839.

Bacterial MEP and carotenoid synthesis

To investigate the presence of the 2-C-methyl-D-erythriol 4-phosphate (MEP) and carotenoid synthesis pathways within the native microbiota of *A. aurita* polyps, sequences of key enzymes at the beginning and end of the respective pathways (*dxs*, *ispC*, *ispA*, *crtE, and crtI*) from representatives of the *A. aurita* microbiota were obtained from the NCBI platform. These sequences were aligned using the Geneious Prime program (version 2020.0.5). Degenerated primers were designed and tested (key resources table) for subsequent use. Therefore, a gradient PCR was conducted to amplify the gene fragments from bacterial DNA, extracted from native and sterile control polyps and native polyps treated with single dose antibiotics and Provasoliś antibiotic mixture using the Wizard Genomic DNA purification kit (Promega, Madison, WI, USA) and the GoTaq® G2 DNA kit (Promega), following the manufacturer's instructions. PCR reactions with successful amplification were purified using the PCR Clean-Up Kit (Machery-Nagel, Düren, Germany).

Illumina sequencing was conducted to identify bacteria within the complex microbial community associated to *A. aurita* capable of performing the MEP pathway and carotenoid synthesis (*dxs, ispC, crtE,* and *crtI*). Bacterial DNA served as template for amplicon library preparation targeting genes from the MEP pathway and carotenoid synthesis (*dxs, ispC, crtE,* and *crtI*) with unique identifier sequences (barcode). Briefly, the primers contained the Illumina adapters (forward: 5'-*AATGATACGGCGACCACCGAGATCTACAC* XXXXXXXX-'3) and (reverse: '5'- *CAAGCAGAAGACGGCATACGAGAT* XXXXXXXX-'3'), indicated by *italics*. Both primers contained an unique eight-base multiplex identifier (indicated as XXXXXXX) to tag the PCR products. Amplification was carried out in a 20 μL PCR reaction with a Phusion high-fidelity DNA polymerase (New England Biolabs) with a cycle of 98°C for 30 sec, followed by 30 cycles (98°C, 9 sec, 55°C, 60 sec, 72°C 90 sec), finalized by a 10 min extension at 72°C. Following, the amplicons were sequenced on an Illumina MiSeq v3 platform. ASVs were then profiled using Kraken2[95] with default settings, against the bacteria RefSeq

complete genomes database made available through kraken2-build (Date of access 05.08.2024). Bracken[96] with a read length of 100 was used to estimate abundances at the family level based on the taxonomic assignments by Kraken2.

QUANTIFICATION AND STATISTICAL ANALYSIS

The recorded number of segments and released ephyrae were shown as mean ± SD. The statistical analysis was performed with a two sample t-test to determine the statistical significance between the average numbers of segments and ephyrae per treatment.